Heliyon 9 (2023) e20484

Contents lists available at ScienceDirect

Heliyon

journal homepage: www.cell.com/heliyon

Research on psychophysiological characteristics of construction workers during consciously unsafe behaviors

Xiangchun Li [a,b], Yuzhen Long [a,*], Chunli Yang [c], Qin Li [d], Weidong Lu [e], Jiaxing Gao [f]

[a] School of Emergency Management and Safety Engineering, China University of Mining and Technology-Beijing, Beijing, 100083, China
[b] State Key Laboratory of Explosion Science and Technology (Beijing Institute of Technology), Beijing, 100081, China
[c] Occupational Hazards Control Technology Center, Institute of Urban Safety and Environmental Science, Beijing Academy of Science and Technology, Beijing, 100054, China
[d] Beijing Shunjinsheng Construction Engineering Supervision Co., Ltd., Beijing, 101399, China
[e] Department of Safety Engineering, Xinjiang Institute of Engineering, Urumqi, 830023, China
[f] Hubei University of Automotive Technology, Shiyan, 442002, China

ARTICLE INFO

Keywords:
Risky psychology
Physiological characteristic
Multiple linear regression
Decision tree regressor
Unsafe behavior prediction

ABSTRACT

Workers' unsafe behavior is a primary cause leading to falling accidents on construction sites. This study aimed to explore how to utilize psychophysiological characteristics to predict consciously unsafe behaviors of construction workers. In this paper, a psychological questionnaire was compiled to measure risky psychology, and wireless wearable physiological recorders were employed to real-timely measure the physiological signals of subjects. The psychological and physiological characteristics were identified by correlation analysis and significance test, which were then utilized to develop unsafe behavior prediction models based on multiple linear regression and decision tree regressor. It was revealed that unsafe behavior performance was negatively correlated with task-related risk perception, while positively correlated with hazardous attitude. Subjects experienced remarkable increases in skin conductivity, while notable decreases in the inter-beat interval and skin temperature during consciously unsafe behavior. Both models developed for predicting unsafe behavior were reliably and well-fitted with coefficients of determination higher than 0.8. Whereas, each model exhibited its unique advantages in terms of prediction accuracy and interpretability. Not only could study results contribute to the body of knowledge on intrinsic mechanisms of unsafe behavior, but also provide a theoretical basis for the automatic identification of workers' unsafe behavior.

1. Introduction

Construction is widely recognized as one of the most hazardous industries worldwide. This industry has experienced higher rates of safety accident than others resulting in a significant number of casualties [1–3]. In the United States, there were over 1000 fatal occupational injuries in construction each year since 2016 [4]. And this number rose to 1075 in 2021, a 37.6% increase since 2011 [4]. The injuries mainly resulted from the falls to a lower level, defined as one of the Construction Focus Four hazards by the Occupational Safety and Health Administration, reported to continue to be the leading cause of work-related deaths, representing more than one in three (34.6%) construction fatalities that year [4]. In the European Union (EU), more than one-fifth (21.5%) of all fatal accidents at

* Corresponding author. Ding No.11 Xueyuan Road, Haidian District, Beijing 100083, China.
E-mail address: cumtblongyz@163.com (Y. Long).

https://doi.org/10.1016/j.heliyon.2023.e20484
Received 9 December 2022; Received in revised form 20 September 2023; Accepted 26 September 2023
Available online 2 October 2023

work took place within the construction industry in 2020, leading the way for all industries [5]. In Norway, construction had the highest share of fatal occupational accidents in 2021 with one-fourth of accidents [6]. Among the reported accidents at work, falls were the type of accident with the largest number accounting for 21.26% [6]. In China, there were 689 fatal accidents in housing and municipal engineering in 2020, resulting in 794 fatalities [7]. According to statistical analysis, falling accidents were the most frequent and caused the highest number of fatalities, accounting for 52.41% and 46.93% of all construction accidents and fatalities respectively between 2017 and 2019 [8]. In recent years, occupational health and safety in construction have been facing serious challenges, which may be primarily responsible for the peculiarities of working activities in this industry, where hazard analysis and safety management are more difficult than in other industries [9].

Working at height is both common and hazardous in construction sites. Statistics indicated that more than 90% of construction work tasks involved working at height, and around 69% of construction accidents occurred in high-risk areas such as scaffolding, holes, or edges [10]. Unfavorable factors in both work and natural environments, such as narrow space and inadequate safety guards, can increase the likelihood of unsafe behavior among workers, ultimately posing threats to their safety and health [11]. Research has shown that workers' unsafe behavior is often the direct or critical cause of construction accidents [12,13]. Haslam et al. [14] also found that human factors contributed to approximately 70% of work-related accidents in construction. And a sample survey revealed that 45.8% $\pm$ 6.4% of construction workers reported their engaging in consciously unsafe behavior [15].

Human unsafe behavior may be committed for many reasons. Usually, it refers to a deliberate but non-malevolent deviation from recommended safety behavior such as safety procedures, regulations, and rules [16,17]. A cognitive model of construction workers' unsafe behavior reveals that human error is produced by five stages including obtaining information, understanding information, perceiving responses, selecting a response, and taking action [18]. Human unsafe behavior is divided into consciously unsafe behavior and unconsciously unsafe behavior [19]. Consciously unsafe behavior comes with a purpose and intention [20,21]. It is perceived to arise under the domination of risk-taking motives in the excessive pursuit of minimized working hours and high outcomes [22,23]. This motivation arises from a combination of individual misjudgment of risk and the team's inability to enforce constraints [23]. It has been demonstrated that time pressure and the presence of other personnel on site were the main contributors to the unsafe behaviors of construction workers [24]. Psychophysiological research has also shown that an individual's motivation, emotion, and cognition can significantly impact their behavior and the ability to adapt to their surroundings [25,26]. This, in turn, can be reflected in physiological activities in an organism.

Following these research clues, our study is focused on the psychological and physiological characteristics during consciously unsafe behaviors. From there, it further aims to explore the potential of significant indictors as predictors for such behaviors. In other words, this study is an attempt to answer the following research question: how to utilize the psychophysiological characteristics to predict the consciously unsafe behaviors of construction workers.

With the goals in mind, we performed an experiment study on consciously unsafe behaviors during working at height. The research approach and route are described in Fig. 1. Firstly, a simulation experiment for working at height was designed and conducted. Then, the risky psychological factors and the physiological characteristics during consciously unsafe behaviors were identified based on statistical analysis. Finally, the significant indicators were utilized to develop prediction models for unsafe behavior based on both methods of multiple linear regression and decision tree regressor.

The remainder of the article is as follows. In Section 2, the research background is discussed. Section 3 presents our research approach, while its results are described in Section 4. Then, Section 5 discusses the results achieved addressing further research work. And Section 6 concludes the article.

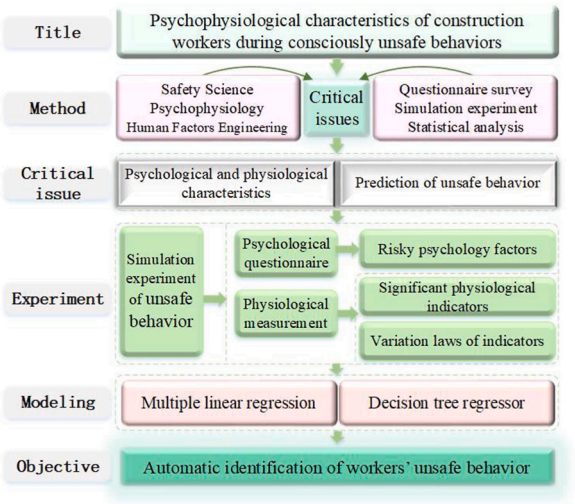

Fig. 1. Scheme of research approach and route.

2. Literature review

Past decades have witnessed that the mechanisms underlying unsafe behaviors were extensively explored from multiple perspectives. For instance, Xingang Yang et al. [20] suggest that consciously unsafe behavior in construction workers is related to safety management and supervision, while Yang [27] identified risk management, immediate supervision, and worker actions as the key causal factors with strong connections. Jingjing Yang [28] presented that psychological and physiological factors interact to influence such behaviors. It was demonstrated that the physiological perceived control strengthened the relationship between safety knowledge and safety behavior [29]. In recent years, there has been a growing focus on exploring the psychological mechanisms underlying unsafe behavior. Rong Cai [30] developed an effective factors model of intentional unsafe behavior, which identified risk perception, external pressure, and safety climate as key factors. Similarly, Jingyi Zhang [31] constructed a risky psychological model, finding that higher levels of risk attitude and lower levels of risk perception were associated with increased scores of in-flight risk-taking behaviors. Yong Ren [32] used the entropy weight method and normal cloud theory to construct a model of landing risk operation propensity evaluation. Meanwhile, Jiang Wu [33] found that safety risk tolerance presented a negative correlation with safety literacy. While research on risky psychology and its impacts on flight risk-taking behaviors has been thoroughly investigated, it is still a relatively underexplored area in the field of building construction.

Studies have shown that physiological signals like electrodermal activity (EDA), heart rate variability (HRV), respiration rate (RESP), and skin temperature (SKT) can serve as indicators of fatigue and stress levels. For example, research by Tian Xiang [34] revealed a positive correlation between task errors and fatigue, which was reflected in the changes in galvanic skin response (GSR), RESP, R–R interval, and SKT. Drivers have also been found to experience heightened nervous with a distinct rise in skin conductance (SC) during overtaking or under the difficult driving conditions such as frozen roads and steep slopes [35]. Similarly, it was revealed that miners' safety capacity and physiological responses like GSR and heart rate (HR) both significantly increase with the severity of fatigue [36]. A psychophysiological measurement experiment revealed that victims experienced intense physiological changes in coal mine accidents, including pulse rate, HR, R–R interval, and RESP [37]. Ronan Doorley [38] found a link between cyclists' subjective risk perceptions and HR while cycling in a mixed mode urban network. The HRV of drivers exposed to stressful scenarios showed a lower-than-normal value while the skin electricity remarkably raised compared to the normal value [39]. Healey and Picard [40] measured physiological responses in drivers to differentiate between mental stress, physical stress, and relaxation. Additionally, Joshi et al. [41] explored the impact of yogic breathing on regulating the GSR of engineering students under stress. It was also revealed that the skin electrical and SKT at high levels were to be a response to positive emotions while the HR at low levels to negative emotions in construction workers [42]. Besides, Mingzong Zhang [43] set up a "danger" zone where subjects had to pass through in the laboratory to investigate the relationship between fatigue and the safety performance of construction workers. In recent years, research on physiological characteristics during fatigue and unsafe behavior has become an emerging focus in the fields of automobile driving and coal mining. Whereas, there has been relatively limited research on this focus in the construction industry.

Domestic and international scholars have obtained fruitful findings which were demonstrated strong energy in the physiological characteristics and fatigue detection of pilots, drivers, and miners. However, the psychophysiological mechanism of unsafe behavior remains in an exploration stage in the construction industry. This study intends to employ commonly used indicators such as HRV, SC, SKT, and RESP in measuring emotional responses to explore the psychophysiological characteristics and effective approaches to predicting unsafe behaviors of construction workers. It would be of great significance to realize the automatic identification of risk-taking propensities and timely rectification of unsafe behaviors for preventing and reducing occupational injuries and accidents caused by human factors in the construction industry.

3. Materials and methods

3.1. Questionnaire survey

The psychological factors that contribute to unsafe behavior among construction workers include personality traits, awareness

Table 1
Questionnaire items.

Indicator	Question item
Task-related risk perception (TRP)	T1. Working at heights is very dangerous. T2. Failure to conduct safety education prior to working at heights tests is not in compliance with the specifications. T3. During the test, the failure to wear safety equipment is not in line with the specifications. T4. The scaffold plate in the test situation poses a safety hazard that should be addressed immediately.
Objective risk perception (ORP)	O1. Safety is paramount in the work process. O2. Safety is relative, and there are potential hazards even when invisible. O3. Safety measures should be given more priority when there is plenty of work to do. O4. Adequate safety protection facilities should be provided at the construction site.
Hazardous attitude (HA)	H1. Safety can be compromised to improve efficiency. H2. The safety belt may not be used when working on lower working surfaces. H3. Working at height without wearing good protective equipment when pressed for time. H4. There is no risk when performing skilled and simple operations. H5. Work at high altitudes on loose scaffolding. H6. No protective measures were set next to the reserved elevator shaft opening. H7. The wires are not led from the distribution box at the construction site. H8. Most tasks can be performed by hand instead of the device. H9. The scaffolding was only one-half laid when working at height. H10. There is no need to invest heavily in safety measures.

levels, cognitive processes, and attitudes toward safety. To measure these factors, we designed and compiled the Risky Psychology Measurement Questionnaire. This questionnaire was developed based on a thorough review of relevant literature and field investigations [31–33,44,45]. The questionnaire consists of several items, which are presented in Table 1.

The questionnaire consisted of three parts, namely TRP, ORP, and HA, each designed to measure a different aspect of risky psychology. A higher score for the first two parts indicated a greater degree of cognition about the risky situation, reflecting a higher level of risk perception. The third part included the dimensions of fluke, blind self-confidence, and risk-taking propensity. A higher score on this part indicated a more dangerous thinking mode and a higher level of HA. The questionnaire was designed using the Likert Scale method, with a score range of 1–5 for each item. Before its administration, the questionnaire underwent a rigorous review process and was approved by five experts in occupational safety and health. This review process helped to ensure that the questionnaire was well-designed and capable of accurately measuring the risky psychological factors.

3.2. Simulation experiment of working at height

3.2.1. Experimental subject

The selection criteria for subjects involved were that they were healthy adult males with no cardiovascular or mental illnesses, no acrophobia, and possessed an understanding of working at heights. Participants were compensated with 20 RMB for their involvement. The optimal sample size was calculated based on the F-statistics by supposing a relative error of 0.05 and an interval probability of 0.9. Given a maximum of seven independent variables for psychological and physiological indictors, the sample size for modeling was supposed to be no less than 45 regarding the minimum sample size criteria established by Ma and Liu [46].

There were 75 volunteer subjects recruited from postgraduates in safety science and engineering, mechanics and civil engineering. This study was conducted in three stages: model construction, parameter validation, and predictive performance analysis, with 50, 15, and 10 subjects, respectively. The participants had knowledge of building construction and some had field investigation experience at construction sites. Their professional knowledge allowed them to make choices similar to those of construction workers. They were aged between 22 and 28 years and in good health. Before the experiment, they were required to maintain a well-regulated daily routine and avoid neurobehaviorally stimulating activities. Besides, they were assured that the study was conducted by university staff with a high level of data anonymity, security, and confidentiality.

3.2.2. Experimental scene

The experiment simulated in a laboratory environment has several advantages over construction sites. It is possible to control extraneous variables in the laboratory by eliminating the interference of other factors that may exist on sites. Besides, there are many challenges in collecting a sufficient number of unsafe behavior samples in a short period at construction sites, while it is more easily implemented in the laboratory. What's more, subjects may be exposed to real dangers at construction sites, which can be avoided by an experimental design in the laboratory.

The experimental design included a simulated platform for working at height, where subjects were induced to behave unsafely. The experimental platform was constructed to resemble a light roof, whose schematic diagram is depicted in Fig. 2. The platform's main body was a hollow pine wood plinth (P) measuring 5 m (m) in length, 1 m in width, and 0.4 m in height. Four load-bearing wooden boards (B1–B4) measuring 1.2 m long and 1 m wide were placed horizontally at each end of the plinth, and a non-load-bearing gypsum board (B5) of the same size was placed horizontally in the middle. The wooden boards were load-bearing and safe for the subjects, while the gypsum board was designated as a "dangerous zone" for potential falling accidents due to its non-load-bearing nature. The wooden and gypsum boards were connected tightly to the plinth using screws. Targeted measures were implemented to reduce the actual risk exposure of the subjects. Anti-collision belts (A) were attached to the edges of the wooden and gypsum boards every 20 cm to keep subjects from falling off the platform. A 0.1m-thick shock-absorbing cushion (C) was placed at the bottom of the plinth to prevent subjects from injuries and a stair (S) was positioned alongside the plinth to allow subjects to board the platform safely.

In addition, the laboratory was maintained at a temperature of 27 °C, a relative humidity of 60%, and a wind speed of 2.6 m/s by a constant temperature and humidity system. These settings were based on statistical data related to natural conditions at a construction site in summer [47].

The task assigned to the subject was to move from a designated starting point to an ending point by passing through the simulated platform for working at height. The width of the gypsum board, that is, the "dangerous zone", was slightly larger than the average stride length of an adult male, making it challenging for the subjects to step over it without dropping from the platform. The subjects tended to undertake risky strides over the "dangerous zone" induced by the rewards and a risk-taking mentality. The risky strides in

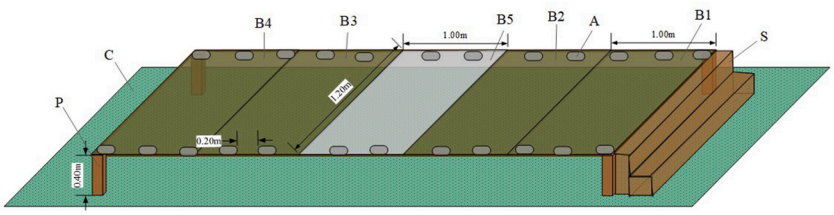

Fig. 2. Schematic diagram of experimental platform.

this way were perceived as consciously unsafe behaviors engaged in by the subjects.

3.2.3. Experimental equipment

ErgoLAB wireless wearable physiological recorders, a multi-parameter integrated sensor system, were employed to collect the physiological signals. Not only can the physiological recorders directly contact the body with minimal restraints, but they also enable wireless data transmission, as depicted in Fig. 3. In recent years, the ErgoLAB wireless wearable physiological recorders have been increasingly employed to study emergency response [48], fatigue detection [49,50], and emotional identification [51].

ErgoLAB human-machine-environment (HME) synchronization cloud platform is equipped with built-in targeted algorithms to pre-process physiological signals, such as filtering, noise reduction, interpolation, and dynamic recognition. The platform includes four modules for the analysis of HRV, EDA, RESP, and general signals. The HRV module mines data information including the mean inter-beat interval (IBI), the standard deviation of N–N intervals (SDNN), the proportion of adjacent N–N intervals with a difference greater than 20 ms (PNN20), the total power (TP), and the low to high frequencies ratio (LF/HF). The EDA module automatically extracts SC through various smoothing processes and performs the analysis of skin conductance reaction (SCR) and skin conductance level (SCL). The RESP module supports deriving the average respiration rate (AVRESP), the standard deviation of respiration rate (RESP Std), and the power of respiration rate (RESP power). The cloud platform allows the presentation of multi-channel data in the same software interface, as shown in Fig. 4.

3.2.4. Experimental process

The experiment was designed following the rules of the Declaration of Helsinki. Each subject signed a written informed consent form for the experiment. The experiment was conducted by the following steps depicted in Fig. 5.

The detailed procedures during the experiment were as follows. To start with, the subjects were informed of experimental tasks and signed an informed consent form, providing permission for their physiological data to be collected for academic research. In the second place, they were assisted in wearing wireless physiological recorders and given 10 min to acclimatize themselves to the recorders. Then, the subjects viewed 10-min videos on working at height and completed a survey on their HAs and ORPs. Afterward, the physiological signals were measured in the subject's natural state, in which they were expected to be emotionally smooth for at least 3 min. What's next, they were guided along a prescribed route to board the experimental platform and undertake their risky strides over the "dangerous zone", that is, consciously unsafe behaviors. Meanwhile, the physiological signals were monitored in real-time during their unsafe behaviors. Followed by, a questionnaire survey was administered to evaluate their perceptions of task-related risks. Finally, the physiological signal data was saved and exported to be processed subsequently. Throughout the experiment, the behavioral video recording was synchronized with the physiological signal acquisition on the ErgoLAB cloud platform, as presented in the supplementary material.

Targeted measures were implemented to minimize potential variations in physiological signals caused by factors other than unsafe behavior. The laboratory was kept quiet during the experiment to avoid dramatic emotional changes in subjects. In addition, the experiments were performed during the same period of 9:00 a.m. and 11:00 a.m. to minimize the impacts of physiological cycles.

The safety of the subjects was a top priority throughout the experiment. Potential risks were thoroughly assessed, and appropriate measures were taken to minimize them. Specially trained assistants were responsible for guiding and attending to the subjects to ensure their safety during the experiment.

3.3. Data pre-processing and analysis methods

3.3.1. Data pre-processing

Before statistical analysis, the physiological signal data were pre-processed using the ErgoLAB HME synchronization cloud

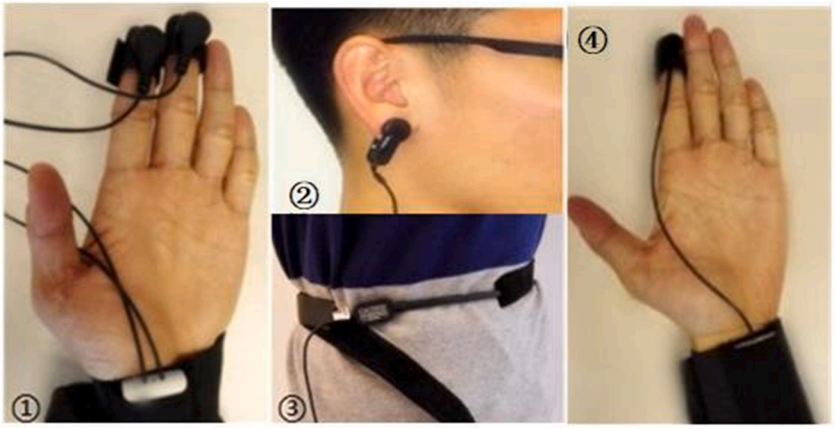

Fig. 3. ErgoLAB wireless physiological recorders.

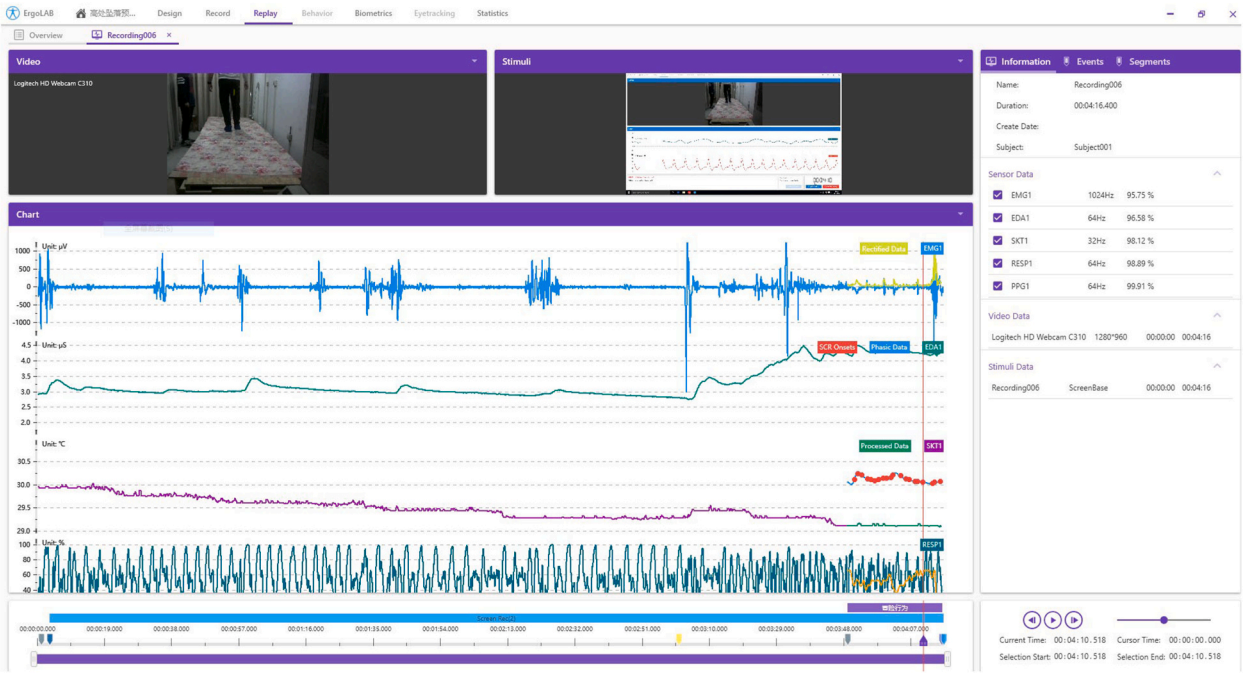

Fig. 4. ErgoLAB HME synchronization cloud platform.

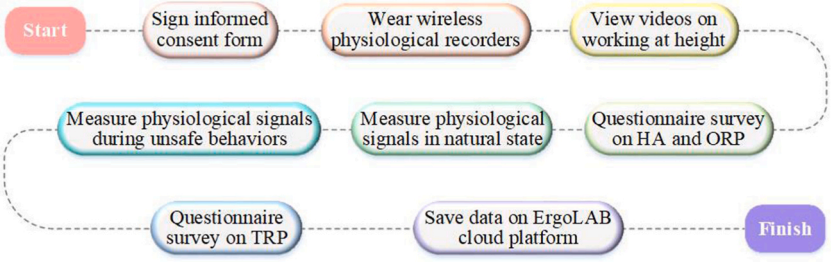

Fig. 5. Scheme of experimental procedures.

platform.

The physiological data for each subject were divided into two segments based on video recording. The baseline segment represented the period during which the subject was monitored for physiological signals in their natural state, while the unsafe behavior segment represented the period during which the subject boarded the simulated platform and undertook their risky strides over the "dangerous zone".

The pre-processing of physiological signals involved four techniques: FFT filters, smoothing, scaling, and resampling. Different signals lend themselves to different techniques. The EDA was subjected to low-pass filtering and Gaussian filtering for its extremely low frequency. The HRV, which was highly susceptible to external noise, underwent low-pass filtering, high-pass filtering, and band-stop filtering. The SKT, which was slightly affected by the external environment, was subjected to the system's default sliding mean filtering. The RESP with a frequency below 10HZ underwent low-pass filtering, band-stop filtering, and sliding mean filtering.

3.3.2. Statistical analysis methods

The psychological factors analysis approach involved questionnaire tests and correlation analysis, as shown in Fig. 6. To assess the reliability and validity of the questionnaire, the survey data were analyzed using IBM SPSS Statistics 26.0. A higher reliability coefficient is associated with a higher degree of consistency in the questionnaire. And a KMO statistic of 0.7 or higher indicated the appropriateness of using exploratory factor analysis (EFA) to validate the questionnaire. EFA would be conducted to extract the common factors of the questionnaire and determine whether it could measure all three assumed dimensions: TRP, ORP, and HA. Afterward, the Pearson correlation analysis was performed to identify the risky psychological factors significantly associated with unsafe behavior.

The physiological characteristics were identified by integrating the normality tests, significance tests, and curve fitting, as

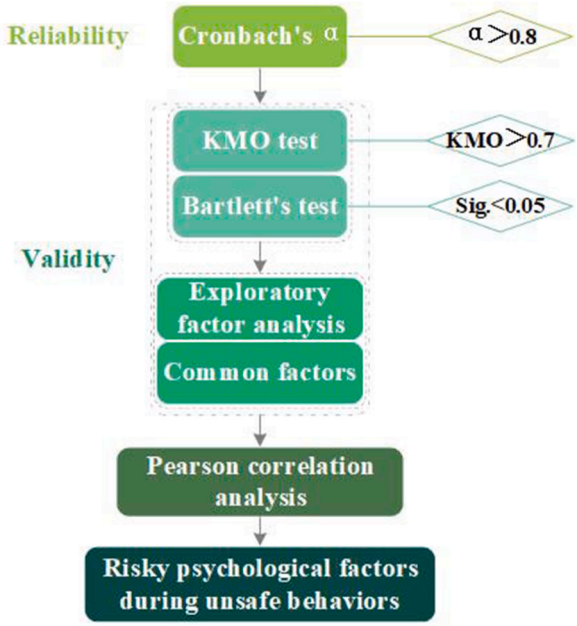

Fig. 6. Scheme of psychological factors analysis approach.

schematized in Fig. 7. The Shapiro-Wilk test was employed to determine the normality of physiological data. The student's t-test was performed for the indicators that followed a normal distribution, while the Wilcoxon rank-sum test was applied for the indicators that were not normally distributed. The null hypothesis for the significance test was that there were no significant differences between the baseline and unsafe behavior segments. If the significance value of the two-sided test was less than 0.05, the null hypothesis would be rejected, which indicated that the values of the indicator for the unsafe behavior segment were significantly different from those for the baseline segment. Curve fitting was then carried out to reveal the variation laws of physiological indicators and determine whether these indicators could serve as valid predictors of unsafe behavior. The fitting model consisted of basic elementary functions such as quadratic function, power function, exponential function, logarithmic function, inverse function, system function, etc.

Following the significance test, prediction models of unsafe behaviors were developed based on both multiple linear regression and decision tree regressor, as depicted in Fig. 8. For the regression analysis, the significant indicators were taken as independent variables

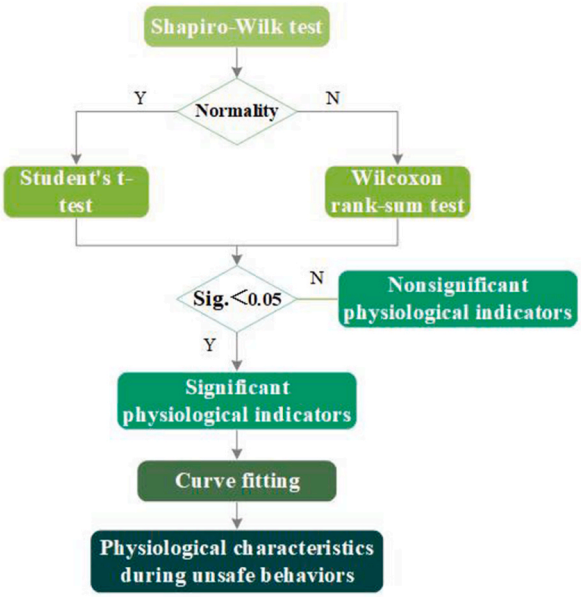

Fig. 7. Scheme of physiological characteristics identification approach.

or input features, while the performance score of unsafe behavior was taken as the dependent variable or output feature. The multiple linear regression coefficients were estimated based on ordinary least squares. The estimates were then tested for significance and examined by the coefficient of determination R^2. Similarly, the decision tree regression model is debugged and optimized in terms of R^2, namely r2_score in the regressor. Finally, the two models were evaluated for their predictive performance.

4. Results and analysis

4.1. Quantification of unsafe behavior performance

To investigate the relationship between consciously unsafe behavior and psychophysiological indicators, it was necessary to quantify unsafe behavior performance (UBP). In a previous study, Jinyi Zhang [31] evaluated flight risk-taking behavior with various indicators such as the grounding speed, minimum descent altitude, fuel consumption, and landing distance measured in a simulated flight experiment. In construction sites, workers tended to be cautious when walking on the working surface at height to prevent falls. Moreover, workers in hazardous situations needed to devote some time, even if briefly, to risk assessment and decision making, resulting in slow movement on the high working surface and long-term pause in front of the danger, which can be considered a performance of the subject's ability to protect themselves from injury.

In this study, the walking speed and residence time before reaching the danger zone were selected as indicators to calculate the score of UBP. The walking speed and residence time of each subject were obtained from the video recording on the ErgoLAB cloud platform. Raw data were provided in the supporting materials. The walking speed and residence time were dimensionless by employing the Z-score standardization method. The mean values of walking speed and residence time were at 0.673 m/s and 2.769s, respectively, with standard deviations of 0.309 m/s and 1.445s, which were then employed as the training parameters for standardization. The standardized data followed a normal distribution. The UBP score was finally obtained by accumulating the two indicators following consistency processing. Table 2 shows the scores of some subjects. A higher score indicated that the subject behaved more dangerously.

4.2. Correlation analysis of risky psychology factors

Reliability and validity tests were conducted on the survey data of the risky psychology questionnaire. The Cronbach's alpha coefficients were 0.919, 0.717, and 0.925 respectively for the dimensions of TRP, OR, and HA, indicating high consistency and reliability of the survey data. The KMO value was 0.777, and Bartlett's spherical test showed a significant approximate chi-square χ^2 of 505.67 with significance at 0.000, which both indicated that the question items were suitable for EFA and strongly correlated with each other. The results of EFA, as shown in Table 3, revealed three common factors with large eigenvalues, which together explained 72.04% of the variance. The loadings of each question item on the belonging common factors were at a high level of 0.6–0.95 with no excessive cross-loadings greater than 0.4 following the rotation by the direct oblique intersection method. The EFA results were consistent with the expected dimensional division results, suggesting that the questionnaire was of good construct validity and that the survey data was favorable for further analysis. Finally, all question items of the three dimensions were retained based on the criterion of factor analysis [52,53].

The correlation analysis between UBP and the three common factors, namely TRP, ORP, and HA, was performed with the Pearson correlation analysis. The analysis results were presented in Table 4. It was observed that there was a significant negative correlation between UBP with TRP, and a positive correlation with HA. However, no significant correlation was found between ORP and UBP. Additionally, there was no significant correlation between TRP and HA.

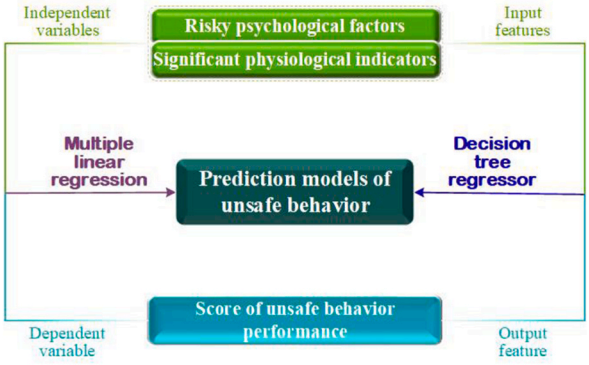

Fig. 8. Scheme of unsafe behavior prediction approach.

Table 2
Scores of unsafe behavior performance (part).

Subject	1	2	3	4	5	6	7	8	9	10	11	12	13	14
ν	0.36	0.39	0.44	0.48	0.5	0.55	0.58	0.68	0.78	0.9	0.96	1.1	1.25	1.36
t	4.55	4.25	4	3.6	3.45	3.15	2.75	2.45	2	1.45	1	0.75	0.55	0.35
Score	−2.25	−1.94	−1.61	−1.20	−1.03	−0.66	−0.29	0.24	0.88	1.65	2.15	2.78	3.40	3.90

Table 3
Results of exploratory factor analysis.

Item	Factor	Communality	Item	Factor		Communality
	F1			F2	F3	
9	0.623	0.388	1	0.933		0.856
10	0.880	0.782	2	0.738	0.332	0.811
11	0.836	0.705	3	0.951		0.856
12	0.734	0.672	4	0.827		0.785
13	0.773	0.575	5		0.632	0.489
14	0.795	0.652	6		0.784	0.578
15	0.731	0.606	7		0.702	0.559
16	0.832	0.697	8		0.732	0.620
17	0.719	0.562				
18	0.727	0.510				
Rotated eigenvalues	6.228			3.598	3.157	
Variance contribution rate	34.6%			19.99%	17.54%	

Note: Loads of <0.3 were hidden.

Table 4
Results of correlation analysis.

Variable	TRP	ORP	HA	UBP
TRP	1	0.446**	−00.033	−0.728**
ORP	0.446**	1	0.311*	−00.197
HA	−00.033	0.311*	1	0.587**
UBP	−0.728**	−00.197	0.587**	1

Note: * denoted $p < 0.05$; ** denoted $p < 0.01$.

4.3. Physiological characteristics during consciously unsafe behavior

4.3.1. Electrodermal activity

EDA is the preferred term for changes in the electrical conductance of the skin, resulting from sympathetic neuronal activity [54]. The Shapiro-Wilk test was utilized to assess the normality of the EDA signals, including SC, SCR, and SCL. The normality test results are presented in Table 5. The p-value for each indicator was all found to be less than 0.05, indicating that none of them followed a normal distribution. Accordingly, the rank-sum test was utilized to evaluate the significance of indicators, and the results are presented in Table 5. The two-tailed significance values were all less than 0.05, demonstrating significant variations in these indicators. The variations in SC, SCL, and SCR were respectively depicted in Fig. 9.

From Table 5 and Fig. 9, it is evident that the SC, SCL, and SCR increased remarkably when consciously unsafe behavior occurred, with the most noticeable variation in SC. To reveal the variation law of the indicator, curve-fitting was performed on the SC within 10 s before and after the occurrence of unsafe behavior. Several curve-fitting models, including the logarithmic function, inverse function, power function, and system function, were selected based on the distribution characteristics of the scatter diagram. The fitting results for SC are presented in Table 6, and the fitted curves are depicted in Fig. 10.

As shown in Table 6, the system function model presented the highest R^2 value of 0.872 and a significant level of Sig.<0.001, indicating its superiority over other models. Therefore, the system function described in Eq. (1) was selected as the EDA regression model for consciously unsafe behavior.

Table 5
Normality and significance test of EDA.

	Normality test			Rank sum test		
	SC	SCR	SCL	SC	SCL	SCR
Z	0.856	0.855	0.933	−5.745	−4.882	−4.529
Sig.	0.000	0.000	0.012	0.000	0.000	0.000

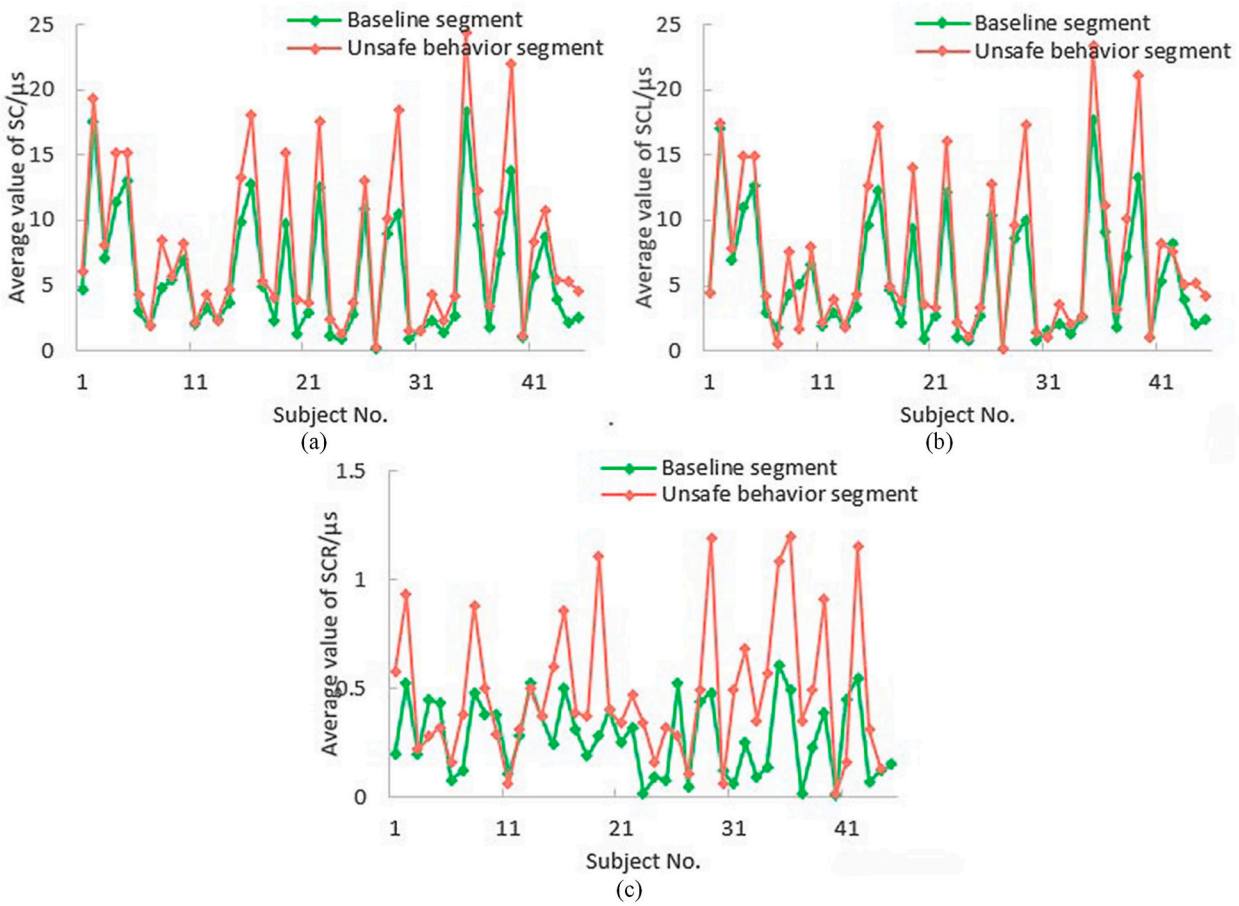

Fig. 9. Variations in EDA indicators: (a) Variations in SC; (b) Variations in SCL; (c) Variations in SCR.

Table 6
Model summary and parameter estimation of SC fitting.

Model	Model summary					Parameter estimation	
	R^2	F	df_1	df_2	Sig.	Constant	b_1
Logarithmic function	0.785	32.819	1	9	0.000	7.718	1.394
Inverse function	0.865	57.686	1	9	0.000	10.635	−2.435
Power function	0.779	31.741	1	9	0.000	7.540	0.169
System function	0.872	61.370	1	9	0.000	2.375	−0.298

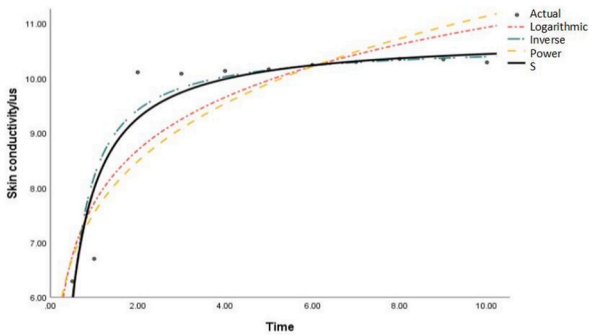

Fig. 10. SC fitting curves during unsafe behavior.

$$y_1 = 1.557t^{0.943} \quad (1)$$

Where t is denoted as the time during consciously unsafe behavior; y_1 denoted as the skin conductance during consciously unsafe behavior.

As observed in Fig. 10, the SC value showed a rapid increase of about 4 μs (μs) within 2 s (s). This suggests that construction workers working at height experience strong sympathetic arousal leading to increased sweat secretion, tension, and anxiety during consciously unsafe behaviors [55]. Thus, SC can be considered as the characteristic indicator that reflects the likelihood of unsafe behavior occurrence.

4.3.2. Heart rate variability

HRV could be quantitatively evaluated for the tension of myocardial sympathetic and vagal nerves [56]. The normality test results are presented in Table 7. The p-value for Mean IBI, PNN20, SDSD, SDNN, and Mean HR was found to be greater than 0.05, indicating that they all followed a normal distribution and could be subjected to t-tests. However, the p-values for TP and LF/HF were less than 0.05, signifying that they did not follow a normal distribution and were appropriate for rank-sum tests. The results of the significance tests are presented in Table 7. The two-tailed significance of Mean IBI, Mean HR, and PNN20 was tested to be less than 0.05, demonstrating significant variations in these indicators. The variations of Mean IBI, Mean HR, and PNN20 are respectively depicted in Fig. 11.

According to Table 7 and Fig. 11, the Mean IBI and PNN20 of the subjects decreased remarkably, while Mean HR increased noticeably. The most notable variation was observed in Mean IBI. Curve-fitting was performed for the Mean IBI with the greatest variation. The fitting results were presented in Table 8, and the fitted curves were depicted in Fig. 12.

As shown in Table 8, the inverse function model best fits the data, with an R^2 value of 0.933 and a significance level of Sig.<0.001. Consequently, the inverse function model represented by Eq. (2) was selected as the HRV regression model for consciously unsafe behavior.

$$y_2 = 480.682 + 305.763\frac{1}{t} \quad (2)$$

Where t is denoted as the time during consciously unsafe behavior; y_2 denoted as the inter-beat interval during consciously unsafe behavior.

As can be seen from Fig. 12, the IBI notably decreased by about 200 ms (ms) within 2s. This indicated that workers had faster heart rate rhythm when consciously unsafe behavior occurred [55]. It could be supposed that the IBI was a good predictor of unsafe behavior.

4.3.3. Respiration rate

The Shapiro-Wilk test was utilized to assess the normality of the respiration signals, including AVRESP, RESP Power, and RESP Std. The normality test results are presented in Table 9. The p-values were all greater than 0.05, indicating that they obeyed normal distributions and could be subjected to t-tests. The significance test results are presented in Table 9. The two-tailed significance of AVRESP and RESP SD were both tested to be less than 0.05, which indicated that there were significant variations in them. The variations of AVRESP and RESP SD are respectively depicted in Fig. 13.

From Table 9 and Fig. 13, it is evident that the AVRESP of subjects increased visibly while RESP SD decreased when consciously unsafe behavior occurred. Given the remarkable variation, the AVRESP was selected for curve-fitting. The fitting results are presented in Table 10, and the fitted curves are depicted in Fig. 14.

As shown in Table 10, the cubic function model best fit the data, with an R^2 value of 00.818 and a significance level of Sig.<0.001. Consequently, the cubic function model represented by Eq. (3) was selected as the RESP regression model for consciously unsafe behavior.

$$y_3 = 14.658 - 0.088t^1 + 0.09t^2 - 0.008t^3 \quad (3)$$

Where, t denoted as the time during consciously unsafe behavior; y_3 denoted as the respiration rate during consciously unsafe behavior.

As can be seen from Fig. 14, the RESP rose by about 1.0 rpm within 2s. It was not considered a reliable predictor of unsafe behavior due to the minor variations observed and the presence of frequent outliers caused by movement status and physical labor.

Table 7
Normality and significance test of HRV.

		Mean IBI	PNN20	SDSD	SDNN	Mean HR	TP	LF/HF
Normality test	Z	0.975	0.979	0.970	0.967	0.953	0.825	0.911
	Sig.	0.442	0.526	0.270	0.203	0.055	0.000	0.002
T-test	t	−13.468	−4.233	0.977	0.195	10.411	–	–
	Sig.	0.000	0.000	0.334	0.846	0.000	–	–
Rank sum test	Z	–	–	–	–	–	−0.322	−0.801
	Sig.	–	–	–	–	–	0.748	0.423

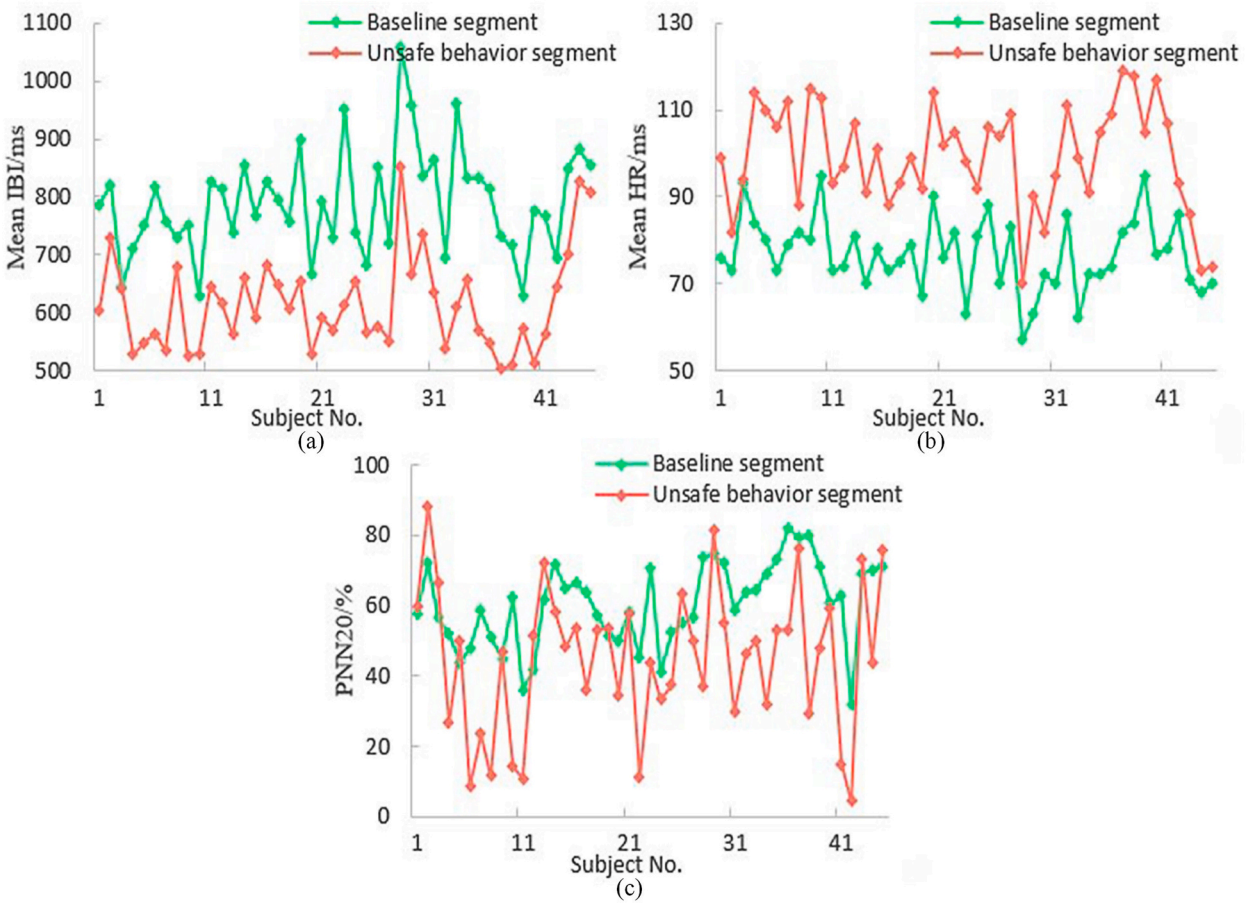

Fig. 11. Variations in HRV indicators: (a) Variations in Mean IBI; (b) Variations in Mean HR; (c) Variations in PNN20.

Table 8
Model summary and parameter estimation of Mean IBI fitting.

Model	Model summary					Parameter estimation		
	R^2	F	df_1	df_2	Sig.	Constant	b_1	b_2
Quadratic function	0.808	25.626	2	12	0.000	789.146	−72.524	4.622
Logarithmic function	0.833	65.038	1	13	0.000	724.761	−104.598	–
System function	0.902	119.151	1	13	0.000	6.195	0.486	–
Power function	0.849	72.941	1	13	0.000	727.777	−1.71	–
Inverse function	0.933	180.323	1	13	0.000	480.682	305.763	–

4.3.4. Skin temperature

The Shapiro-Wilk test was utilized to assess the normality of the SKT signals, including Mean SKT and SKT Std. The normality test results are presented in Table 11. The p-values were all greater than 0.05, indicating that they obeyed normal distributions and could be subjected to t-tests. The significance test results are presented in Table 11. The two-tailed significance of SKT Mean and SKT Std were both tested to be less than 0.05, demonstrating significant variations in them. The variations of SKT Mean and SKT Std are respectively depicted in Fig. 15.

From Table 11 and Fig. 15, it is evident that both the SKT Mean and SKT SD decreased as consciously unsafe behavior occurred. Given the notable variation, the SKT Mean was selected for the curve-fitting. The fitting results of SKT are presented in Table 12, and the fitted curves are depicted in Fig. 16.

As shown in Table 12, the cubic function model best fits the data, with an R^2 value of 0.766 and a significance level of Sig.$<$0.001. Consequently, the cubic function model represented by Eq. (4) was selected as the SKT regression model for consciously unsafe behavior.

$$y_4 = 36.011 - 0.307t^1 + 0.049t^2 - 0.002t^3 \tag{4}$$

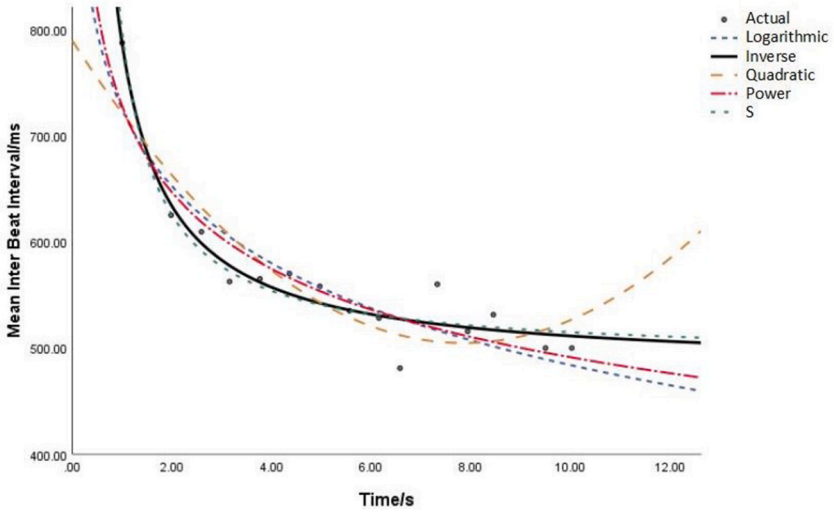

Fig. 12. Mean IBI fitting curves during unsafe behavior.

Table 9
Normality and significance test of RESP.

	Normality test			T-test		
	AVRESP	RESP Power	RESP Std	AVRESP	RESP Std	RESP Power
Z/t	0.976	0.972	0.953	2.573	−2.893	−0.758
Sig.	0.416	0.323	0.053	0.014	0.007	0.453

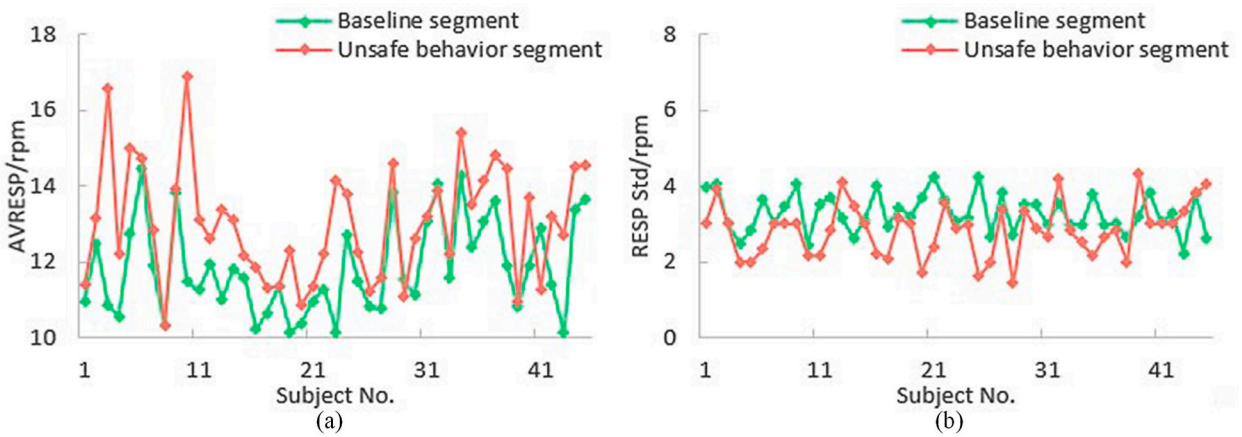

Fig. 13. Variations in RESP indicators: (a) Variations in AVRESP; (b) Variations in RESP Std.

Table 10
Model summary and parameter estimation of RESP fitting.

Model	Model summary					Parameter estimation			
	R^2	F	df_1	df_2	Sig.	Constant	b_1	b_2	b_3
Linear function	0.561	197.728	1	155	0.000	14.692	0.122	–	–
Logarithmic function	0.525	171.081	1	155	0.000	14.842	0.351	–	–
Quadratic function	0.724	201.767	2	154	0.000	14.268	0.377	−0.026	–
Cubic function	0.818	229.465	3	153	0.000	14.658	−0.088	0.090	−0.008

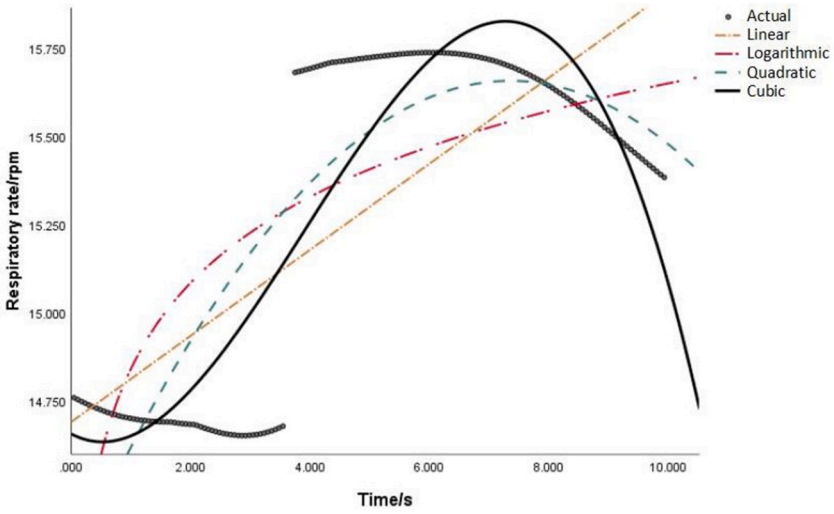

Fig. 14. AVRESP fitting curves during unsafe behavior.

Table 11
Normality and significance test of SKT.

	Normality test		T-test	
	Mean SKT	Std	Mean SKT	Std
Z/t	0.982	0.985	−3.822	−7.113
Sig.	0.721	0.818	0.000	0.000

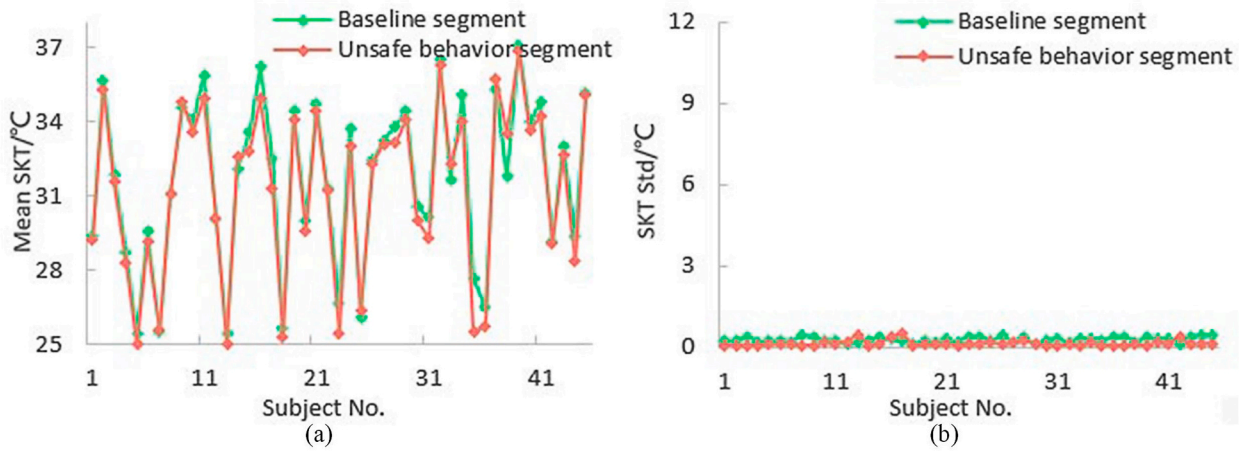

Fig. 15. Variations in SKT indicators: (a) Variations in Mean SKT; (b) Variations in SKT Std.

Table 12
Model summary and parameter estimation of SKT fitting.

Model	Model summary					Parameter estimation			
	R^2	F	df_1	df_2	Sig.	Constant	b_1	b_2	b_3
Inverse function	0.612	489.410	1	310	0.000	35.401	0.326	–	–
Quadratic function	0.523	169.514	2	309	0.000	35.756	−0.102	0.008	–
Cubic function	0.766	335.247	3	308	0.000	36.011	−0.307	0.049	−0.002
System function	0.612	488.391	1	310	0.000	3.567	0.009	–	–

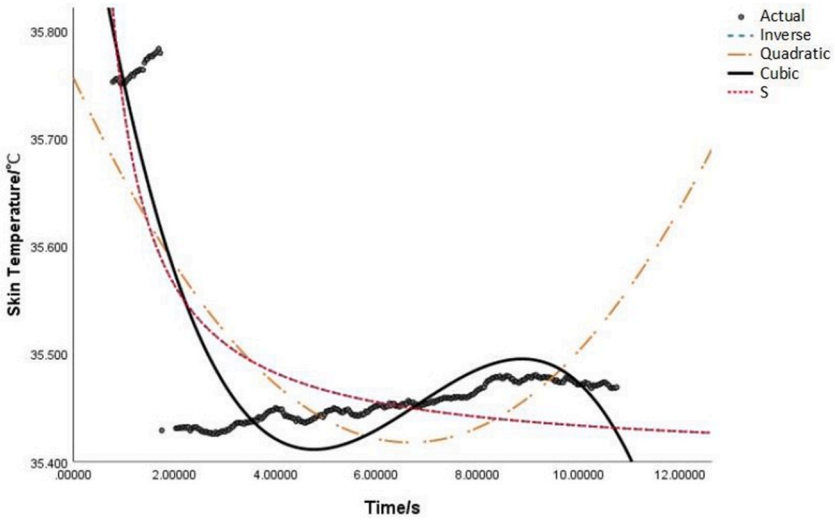

Fig. 16. Mean SKT fitting curves during unsafe behavior.

where t is denoted as the time during consciously unsafe behavior; y_4 denoted as the skin temperature during consciously unsafe behavior.

As can be seen from Fig. 16, the SKT reduced instantly by 0.4 °C within 2s. The changes might be responsible for the increased sweat secretion in response to emotional changes such as tension, anxiety, and stress. The SKT could be regarded as a promising candidate for the prediction of consciously unsafe behavior.

4.4. Prediction models of unsafe behavior performance

4.4.1. Multiple linear regression model

It was observed that UBP exhibited a statistically significant correlation with two risky psychological factors, namely TRP and HA, as well as three physiological indicators, namely SC, IBI, and SKT. The original multiple linear regression (MLR) model was developed by taking the UBP score of the original sample as the dependent variable, while the TRP, HA, SC, IBI, and SKT as independent variables. The parameters for the original MLR model are presented in Table 13.

To ensure the reliability of the parameter estimation, a statistical hypothesis test was conducted on the original MLR model. The adjusted coefficient of determination $\overline{R^2} = 0.97$, which indicated that the variation of the dependent variable was strongly explained by the independent variables. The statistic of the F-test, $F = 237.594 > F_{0.05} = 3.687$, revealed that there was a significant linear relationship between the independent and dependent variables.

The original MLR model was validated for stability and sensitivity to the changes in sample size. To do this, an additional 15 subjects who had not previously participated in the original experiment were included in the analysis, resulting in an expanded sample from the original sample. A new model, called the super-sample MLR model, was developed by re-estimating the parameters using the expanded sample. Given that the parameters β both followed normal distributions, a *t*-test was employed to evaluate the significance of the differences between the β original and super-sample MLR models. The expectation was to find that the difference between the two models was not significant. The results of the significance test for parameter estimation are presented in Table 13.

The p-value of the *t*-test was sig. $= 0.9 > 0.5$, indicating that there was no significant difference between the β original and super-sample MLR model. Therefore, the original MLR model was regarded to have passed the parameter test and expressed as the following equation (5):

Table 13
Parameter estimations of MLR model.

Variable		Original model				T-test		Super-sample model			
		β	Std.	t	Sig.	t	Sig.	β	Std.	t	Sig.
TRP		−0.342	0.145	−2.327	0.025	−0.134	0.900	−0.341	0.118	0.118	0.006
HA		0.334	0.115	2.857	0.007			0.330	0.092	0.092	0.001
SC		0.570	0.244	2.345	0.024			0.554	0.204	0.204	0.009
Mean IBI		−0.463	0.216	−2.132	0.039			−0.454	0.181	0.181	0.015
SKT		−0.496	0.201	−2.495	0.017			−0.489	0.154	0.154	0.002
Normality test	Z	0.826						0.824			
	Sig.	0.130						0.125			

$$y = -0.342x_1 + 0.334x_2 + 0.570x_3 - 0.463x_4 - 0.496x_5 \quad (5)$$

where, x_1 denoted as task-related risk perception; x_2 as hazardous attitude; x_3 as the variation of skin conductance; x_4 as the variation of the inter-beat interval; x_5 as the variation of skin temperature; y as an unsafe behavior performance score.

The prediction performance was tested to determine whether it could be adopted for a wide range of individuals. There were ten subjects other than the modeling samples selected as prediction samples. Following the standardization by the training parameters, the MLR model was used to obtain predicted UBP scores for the prediction samples, as shown in Table 14.

4.4.2. Decision tree regression model

The decision tree regressor was employed to perform regression analysis on UBP. The decision tree regression (DTR) model was developed by taking UBP as output features and TRP, HA, SC, IBI, and SKT as input features. To split the data, 80% of the expanded sample was randomly assigned as a training set, while the remaining 20% was used as a validation set by the train_test_split function built-in to the Scikit-learn library. The prediction sample was treated as a test set for the regression analysis. The original DTR model was developed by the default parameters built-in to the decision tree regressor. The model needs to be debugged due to its poor R^2 performance, as indicated by an r2_score of only 0.5 on the test set. During the debugging process, it was observed that the model showed a higher r2_score when the random_state was set to 13 for the train_test_split function. As such, the training set obtained by splitting the samples under the parameter condition of random_state = 13 was selected for further debugging of the original model. The DecisionTreeRegressor function's parameters, namely random_state and min_samples_leaf, were then fine-tuned. The model's performance was evaluated using r2_score on the test set as an indicator of quality. Fig. 17 displays the optimization process for the original DTR model.

The optimal values for the parameters random_state and min_samples_leaf were both determined as 1, as shown in Table 15. These parameter values were used to develop the optimal DTR model, which yielded a maximum r2_score of 0.86 on the test set. The r2_score on the training set was 1, indicating that the model captured the variations in the output feature very well. The r2_score on the validation set was 0.819, which suggests that the model was of relatively high reliability. Overall, the results indicate that the regression relationships in the DTR model are strong and explain a substantial portion of the variation in the output feature.

5. Discussion

5.1. Implications of psychological and physiological characteristics

The study results revealed a significant negative correlation between TRP and UBP, as well as a positive correlation between HA and UBP. These findings are consistent with the results of Cai Rong's study on the factors influencing intentionally unsafe behavior in construction workers [30]. It was also found that ORP, which is unrelated to the task situation, did not have a significant impact on unsafe behavior. This indicated that risk perception is of "situation specificity", whose connotation may change with risk situations [31]. That is why risk perception, a social cognitive variable, is more variable and immediate than personality traits. In contrast, the HA consistently exerts a significant positive influence on unsafe behavior regardless of the change in risk situations. This indicates that HA is more "situationally transferable" [31]. Consequently, it is crucial to provide education and training to enhance r workers' risk perception and safety literacy to prevent consciously unsafe behaviors.

Some physiological indicators showed significant changes during consciously unsafe behaviors, with SC sharply increasing by about 4 μs, IBI rapidly decreasing by about 200 ms, and SKT reducing by around 0.4 °C instantly. Similar findings were also reported in studies on transportation and aviation industries. For instance, it was reported that drivers who experienced an accident in a risky situation exhibited a greater rise in SC than drivers who did not encounter any risky situation [57]. Similarly, in aviation, pilots showed a significant increase in SC during critical flight situations, such as when the aircraft encountered turbulence or when the pilot made a mistake [58]. Furthermore, Wang Lei and Gao Shan found that IBI presented a declining trend with an increase in adventure flight time [35]. These findings suggest that changes in SC, IBI, and SKT may serve as physiological indicators of consciously unsafe behaviors in various industries.

5.2. Exploration of the psychophysiological mechanisms of unsafe behavior

The decision-making process of risk-taking behavior is mediated by various brain regions. Previous studies have reported negative

Table 14
Prediction performance of MLR model.

Subject	1	2	3	4	5	6	7	8	9	10
True score	−1.67	−1.09	−0.65	−0.45	−0.01	1.429	1.664	2.306	2.93	3.439
Predicted score	−1.71	−1.24	−0.77	−0.51	−0.03	1.387	1.625	2.415	3.079	3.538

The results of the *t*-test showed that there was no significant difference between the true and predicted scores, with sig. = 0.99 > 0.5. Furthermore, the coefficient of determination R^2 for the prediction sample was 0.997, indicating that the MLR model was of superior goodness of fit and high accuracy for prediction.

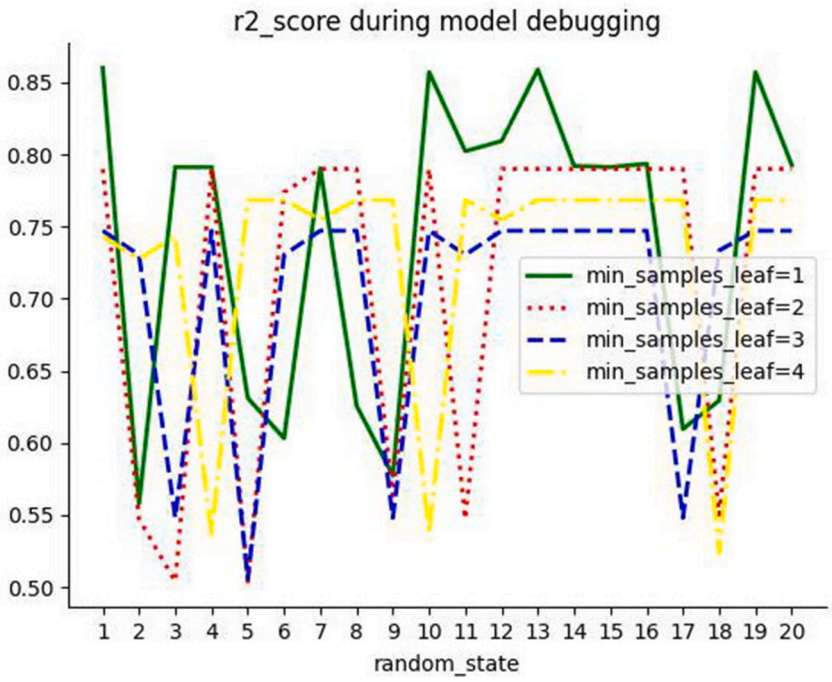

Fig. 17. Optimization process for original DTR model.

Table 15
Parameter values of optimal DTR model.

Parameter	Value	Parameter	Value	Parameter	Value
criterion	'squared_error'	max_leaf_nodes	None	min_samples_split	2
max_depth	None	min_impurity_decrease	0.0	random_state	1
max_features	None	min_samples_leaf	1	splitter	"best"

correlations between risk-taking behavior and grey matter volume in specific brain regions such as the amygdala, striatum, hypothalamus, and dorsolateral prefrontal cortex [59]. These associations may arise from the functional connectivity and coupling between these regions [60–62]. The prefrontal cortical (PFC) plays a crucial role in the processing of emotional information related to cognition and fear. Differences in impulsive control among individuals with or without risk proneness can be attributed to the neural basis provided by the PFC [63]. It sends signals to the hypothalamus, grey matter surrounding the cerebral aqueduct, and striatum [64]. Then, the substantia nigra in the basal ganglia releases dopamine (DA) to the striatum for potential reward prediction. The relationship between cognitive performance and dopamine levels follows an inverted U-shaped function [65]. The nucleus accumbens D2R NAc cells can control the online selection of risky options and decision-period activity in these cells causally drives risk-preference [66]. If the brains of individuals have fewer or less functional D2 receptors, their dopamine release is poorly regulated and disproportionately at high amounts. Excessive accumulation of dopamine signals the brain that the rewards requiring more time are simply not worth waiting for and makes the individuals become much heavier discounters of the delayed rewards [67]. The discounters tend to shift their preferences toward the immediate rewards with more impulsiveness and behave themselves impulsively with little foresight [68]. In addition, the hypothalamus stimulates the pituitary gland to secrete endorphins (END), which can provoke harm-avoidance behaviors in the body. As pointed out by Bill Bryson, "When you exercise vigorously, the pituitary gland squirts endorphins into your bloodstream." Endorphins are known to induce feelings of euphoria and stimulate the mind, which is considered a reward by the brain for successfully avoiding danger. To prevent the reduction of these rewards, the pituitary gland may release a continuous flow of endorphins. During moments of mental flow required for survival, the surge of endorphins may significantly amplify the level of behavioral excitation, resulting in an increased propensity towards impulsive actions to experience a momentary pleasure. For instance, this may motivate an organism to continue high-intensity exercise or engage in risk-taking behaviors. Furthermore, the activation of 5-hydroxytryptamine secreted by the raphe nuclei in the upper pons and midbrain inhibits behaviors such as violence, anger, risk-taking, and aggression. The neurophysiological basis of decision-making for risk-taking behavior is briefly depicted in Fig. 18.

Behavioral responses are controlled by the somatic nervous system, which is under the regulation of the central nervous system. The PFC plays a crucial role in decision-making by transmitting signals to the cerebellar cortex, which is responsible for planning and programming movements. Nerve fibers from the cerebellar cortex then project to the cortical motor area via the pons, dentate nucleus,

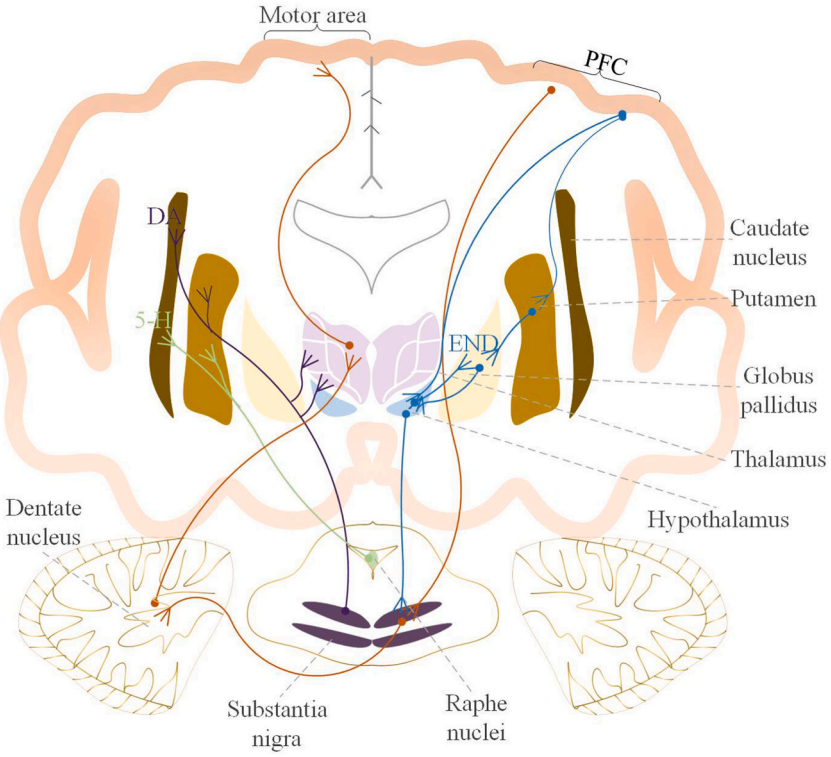

Fig. 18. Neurophysiological basis of decision-making on risk-taking behavior.

and ventral lateral nucleus of the thalamus. The motor area, in turn, sends instructions to the pyramidal system, which innervates the skeletal muscles through the corticobulbar tract and the corticospinal tract to execute behavioral movements. The conduction pathway of the pyramidal system is illustrated in Fig. 19. Additionally, the substantia nigra in the extrapyramidal system secretes dopamine to the striatum, which drives motor coordination. Furthermore, dopamine can be converted to norepinephrine, which enhances somatic performance during stress and movement.

During the stress response, the PFC is also closely linked to the amygdala in the limbic system. The amygdala, which links the brain stem and spinal cord in a downward direction, plays an essential role in emotional regulation. The psychophysiological mechanism of risk-taking propensity is depicted in Fig. 20. The intermediolateral nucleus in the grey matter of the spinal cord is the low-level center of the sympathetic nervous system. The preganglionic fibers originate from the lateral horn of grey matter, and exit the spinal nerve through the intervertebral foramen. They then enter the ganglion of the sympathetic trunk via white communicating branches. After some preganglionic fibers re-permute within the ganglia, their postganglionic fibers leave the sympathetic trunk and return to the spinal nerve via grey communicating branches. From there, they are distributed to various effectors such as blood vessels, sweat glands, and the arrector pili muscle of the limbs and body wall. The preganglionic fibers innervate the adrenal medulla to release acetylcholine (Ach) at the presynaptic cholinergic neuron ending. Ach then binds to M3 receptors on the surface of hyaline cells in exocrine sweat glands, activating chloride channels in the cell membrane and calcium channels on the luminal surface. This creates a negative potential difference that attracts sodium ions, ultimately leading to psychogenic sweat secretion. The sweat ducts within the skin can be regarded as a set of variable resistors connected in parallel, with each having a conductivity related to the proportion of sweat in the duct. The increased sweat secretion leads to decreased resistance, causing fluctuations in the SC [69]. When sweat fills the duct and overflows, the SC rapidly rises, followed by a return to normal levels within seconds as the sweat is reabsorbed or evaporates. Another portion of the preganglionic fibers is then distributed with arterial plexus to various effectors, including the heart and glands, after the intra-neural re-permutation. The preganglionic fibers also innervate the adrenal medulla to release adrenaline and noradrenaline (NA). The NA can strongly activate α receptors, leading to blood vessel constriction. It also stimulates β receptors, enhancing myocardial contraction and increasing cardiac ejection. Both of these effects can raise coronary blood pressure and decrease IBI. Additionally, the excitation of the sympathetic nervous system can also cause changes in SKT, along with SC and HRV. The evaporation of sweat can remove heat, which in turn reduces the SKT. Studies have shown an inverse association between SKT, especially in distal regions, and ambulatory blood pressure [70].

The psychophysiological mechanisms underlying consciously unsafe behavior provide a valuable explanation for the experimental results from a neurobiological perspective. The role of dopamine in reward prediction and endorphins in inducing euphoria may significantly influence the decision-making of risk-taking behavior. The study by Jun Kitazono et, al [71]. revealed that the network cores with strong bidirectional connections were rather concentrated in the iso-cortical regions and thalamic regions, supporting this

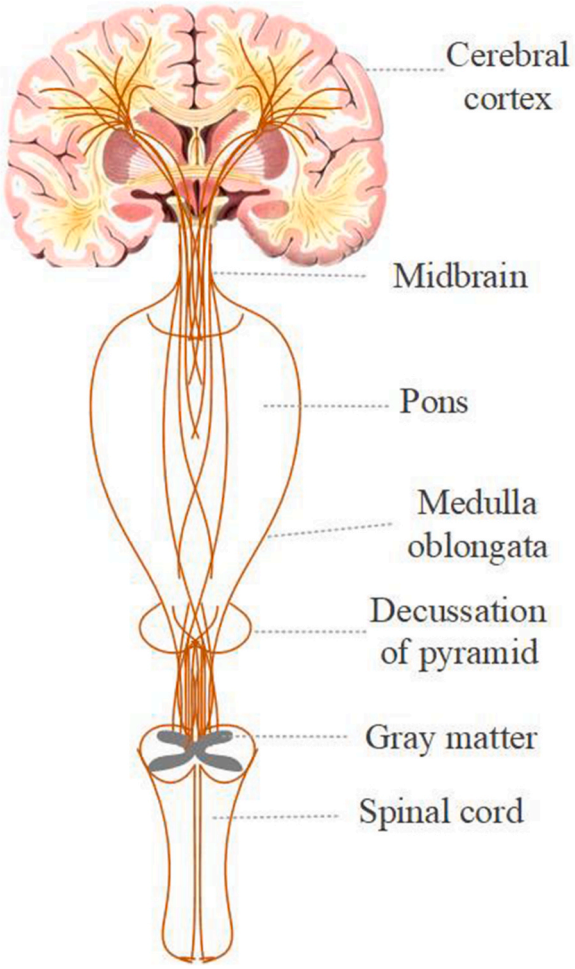

Fig. 19. Conduction path of the pyramidal system.

inference. However, further verification through controlled experiments is required to confirm the role of dopamine and endorphins in inducing risk-taking behavior, as well as to explore the potential influence of other neurotransmitters and hormones. Stronger task-belief is associated with better perception and better discriminability of believed-relevant features [72], which is a critical factor in behaviors that could lead to unsafe outcomes. It can be used as an indicator for personality trait selection, safety literacy development, and safety performance assessment in the safety management of the construction industry.

The propensity for risk-taking can trigger a physiological stress response through the activation of the sympathetic nervous system, which can alter levels of Ach and NA and then impact SC, HRV, and SKT. However, genetic and medical factors may contribute to variations in these substances among individuals, raising questions about how to quantify the relationship between changes in their levels and physiological indicators during risk-taking decision-making. Understanding the impact of these variations on behavioral prediction is also an important area for an investigation to improve the generalizability and accuracy of identifying unsafe behavior.

5.3. Performance evaluation of UBP prediction models

The R^2 is a commonly used metric to assess the adequacy of regression models. The MLR model achieved an R^2 greater than 0.9 on both the original and expanded samples, and even reached 0.997 on the prediction samples, indicating a reliable and well-fitted model. However, the DTR model showed an R^2 of 0.819 on the validation set, which represents a difference of 0.181 compared to the 1.00 achieved on the train set. This difference suggests the possibility of slight overfitting which was fortunately not significant. Despite this, the DTR model still demonstrated an R^2 of 0.86 on the test set, indicating a satisfactory level of goodness of fit.

In addition to R^2 , there are several other metrics used to evaluate regression performance: mean squared error (MSE), mean absolute error (MAE), and explained variance score (EVS). Table 16 shows the values of these metrics for both the MLR and DTR models on the test set. Both MSE and MAE are less than 0.5, indicating that the models have small prediction errors for features' values. Specifically, the MLR model presents lower MSE and MAE, indicating higher prediction accuracy compared to the DTR model. All EVS values exceeded 0.8, indicating that the variations could be mostly explained by the regression relationship between output and input

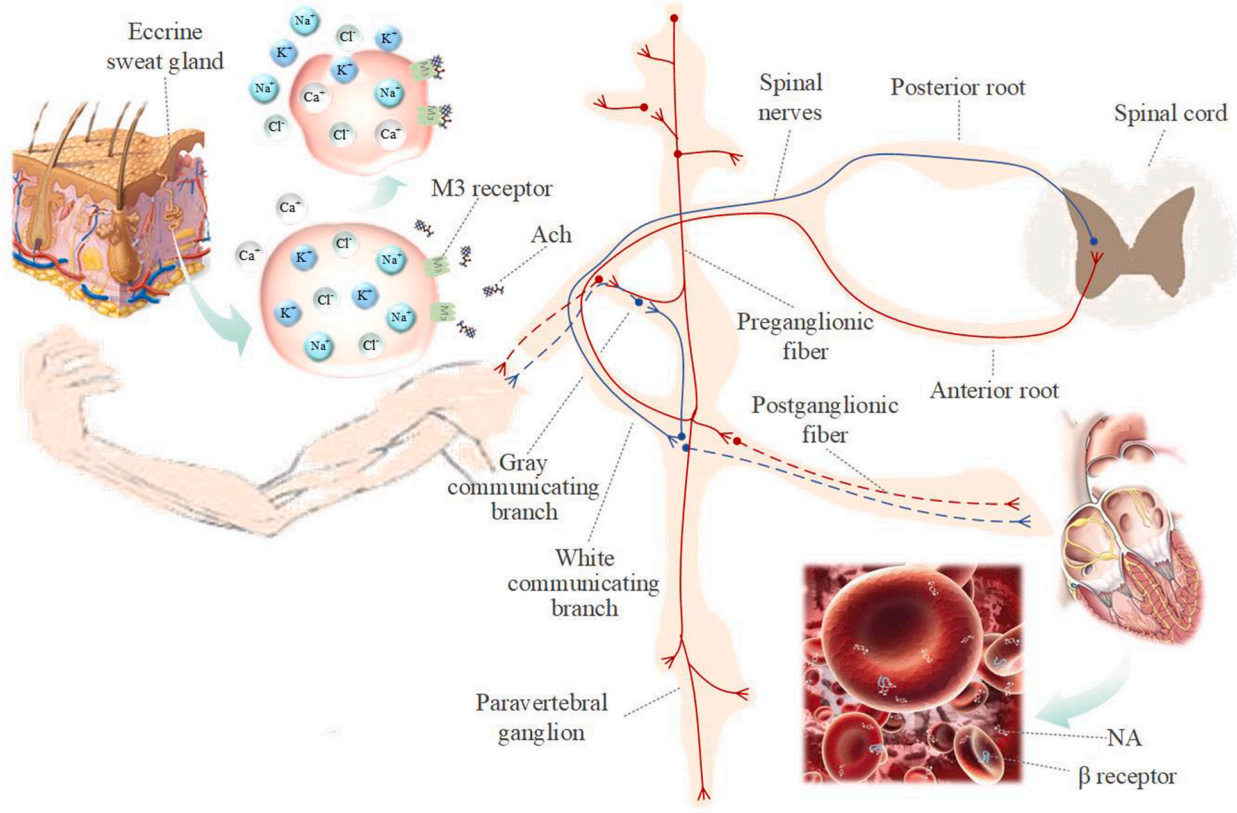

Fig. 20. Psychophysiological mechanism of risk-taking propensity.

Table 16
Regression metrics of prediction models.

Metrics	MSE	MAE	EVS
MLR	0.009	0.0830	0.9969
DTR	0.4042	0.4785	0.8685

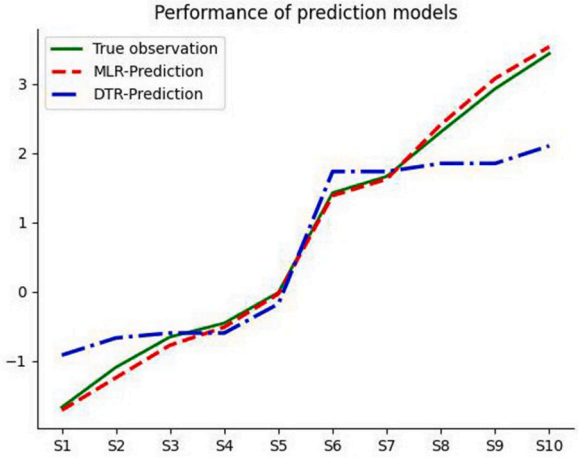

Fig. 21. Performance of prediction models.

features. However, the slightly lower EVS for the DTR model suggests that although it fits most values of features relatively well, it may not fit the distribution of features exactly enough, which can lead to deviations between predicted and true values. This deviation is more evident when comparing the predicted and true values in Fig. 21, where it is clear that the MLR model's prediction values follow the fluctuation trend of the true observation values more closely. Overall, the MLR model has a slightly better prediction performance compared to the DTR model.

However, the MLR model may be slightly less effective when it comes to outlier handling. In this study, the confounding factors outside of risky situations were minimized as much as possible to precisely capture the psychophysiological characteristics of risk-taking propensity during the experiment. In a real-world environment, however, these confounding factors potentially cause extreme changes in physiological signals, leading to abnormal values. The MLR model may be highly responsive to such outliers, as it relies on linear correlations among variables [73]. Consequently, the MLR model may be better suited for workers in calmer workplaces, while the DTR model, which is less sensitive to outliers [74], may perform better perform unsafe behaviors in a noisy environment.

5.4. Application of unsafe behavior prediction model

The prediction models for unsafe behavior provide valuable insights for the development of a physiological monitoring and warning system, which could significantly improve construction safety management. The schematic diagram of the monitoring system is presented in Fig. 22.

The workers' physiological signals, such as EDA, HRV, SKT, and RESP, are monitored using smart wearable physiological sensors built into their helmets or workwear. The sensors transmit real-time physiological data to a cloud-based synchronization platform that is integrated with the prediction models. In case the UBP score of a worker surpassed exceeds a predetermined threshold value (e.g., 2), the cloud platform will activate the alarm system and send out warnings to alert the worker. Noteworthy is that the thresholds are supposed to be dynamically adjusted to account for any potential changes in the work environment. Additionally, the data should also be transmitted to a supervision system to enable managers to keep track of workers' safety performance and implement further safety management measures.

The integration of a physiological monitoring system can serve as a valuable tool in rectifying the motivations of unsafe behaviors and has the potential to revolutionize safety training methods. This technology can be utilized to evaluate workers' UBP in near-realistic high-risk situations created by VR technology. Using the UBP score, targeted interventions can be implemented to enhance the safety literacy of workers. The application of the physiological monitoring system, combined with the developed prediction models of unsafe behaviors, holds significant promise in preventing and reducing occupational injuries and accidents caused by human factors in the construction industry.

5.5. Analysis of experimental limitations

The developed prediction models are mainly applicable to young construction workers, in view that the subjects in the experiment were the postgraduates whose mean age was slightly lower than that of workers actively working on the construction site. However, it was revealed that older subjects (mean 65 years old) had a significantly lower electrodermal response (EDR) than younger subjects (mean 24 years old) in the operational condition, indicating a tendency for lower arousal levels and faster adaptation [75]. Despite the age difference, the subjects in this experiment were still relatively representative as they possessed engineering expertise and internship experience. In addition, we have endeavored to simulate a platform for working at height, such as a light roof, in which the subjects would be inclined to engage in unsafe behaviors. The experimental simulations might be slightly different from a real construction site environment. For future research, it would be worthwhile to explore the use of virtual reality technology to create a more

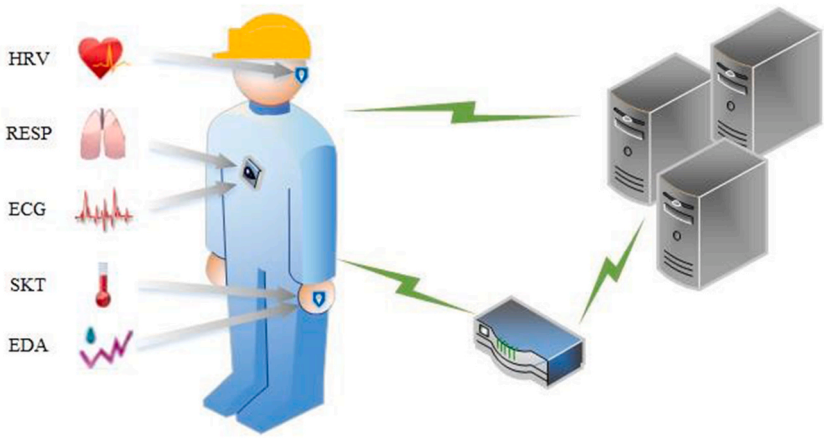

Fig. 22. Schematic diagram of physiological monitoring system.

real scene of a construction site environment.

The identification of unsafe behavior may be influenced by a variety of factors. Scholars have reported that there were significant differences in drivers' eye movement in hazardous situations compared to safe situations [35,76]. The EEG was recognized to have a greater impact on emotion than other indicators [77]. To improve the accuracy and reliability of the prediction model, eye movements and EEG can be integrated into the model to identify and correct workers' unsafe motivation timely and to have more adequate emergency response time. In additional, physical fatigue and environmental factors were not considered in the analysis restricted by the experiment cycle. However, as Yu Zhang [36] reported, the maximum EDR value of workers tends to increase with fatigue. It was also revealed by Jing Li [51] that accidents tended to increase when the minimum illumination level was below 10lx. Accordingly, the identification and early warning of unsafe behavior would be more reliable and effective if the fatigue and environmental changes were integrated into the experimental scenes. Moreover, the psychological mechanisms of unsafe behaviors warrant in-depth study from the perspective of personality traits, emotional states, and professional qualifications to prevent accidents by taking psychological intervention measures. Last but not least, more sophisticated and novel methods deserve to be employed to improve the accuracy and stability of model prediction, such as support vector machine and back propagation neural network. It is promising to achieve the automatic identification of the distraction, stress, and fatigue of construction workers, as well as the early warning of their unsafe behavior.

6. Conclusion

This study explored the psychological and physiological characteristics of consciously unsafe behaviors and how to predict such behaviors by utilizing those characteristics. The conclusions are mainly obtained as follows.

(1) Unsafe behavior performance is strongly associated with TRP and HA. Accordingly, it is suggested that safety education and training programs focus on how to improve workers' perceptions of task-related risks. And innovative means such as case video and virtual reality should be utilized to enhance workers' safety literacy.
(2) Some physiological indicators showed significant changes during consciously unsafe behaviors, with SC sharply increasing by about 4 μs, IBI rapidly decreasing by about 200 ms, and SKT reducing by around 0.4 °C instantly. The decision-making process of risk-taking behavior is mediated by various brain regions. The role of dopamine in reward prediction and endorphins in inducing euphoria may significantly influence the decision-making of risk-taking behavior. The risk-taking propensity induces the excitation of the sympathetic nervous system, resulting in a physiological stress response. Ach and NA are the essential substances responsible for the changes in the SC, HRV, and SKT in the stress response. The interaction pattern of neurotransmitters and hormones in an organism may be a critical issue for the inherent mechanisms of unsafe behaviors to further promote occupational health and safety in the construction industry.
(3) The MLR and DTR models both showed excellent predictive performance for unsafe behaviors, achieving MSE and MAE values of less than 0.5. These models can be integrated into a psychophysiological monitoring system to facilitate the detection and early warning of workers' unsafe behaviors. However, each model has its own strengths in terms of accuracy and interpretability. The choice of model should depend on the specific needs of the situation. With the aid of these models, it is promising for the automatic identification of risk-taking propensities and timely rectification of unsafe behaviors, ultimately preventing and reducing the occupational injuries and accidents caused by human factors in the construction industry.

Funding

This work was supported by the Ministry of Education of the People's Republic of China Humanities and Social Sciences Youth Foundation, China [grant number 19YJCZH087]; the Opening Project of the State Key Laboratory of Explosion Science and Technology (Beijing Institute of Technology), China [grant number KFJJ22-15M]; the National Natural Science Foundation of China [grant number 52274245]; the Fundamental Research Funds for the Central Universities, China grant number [grant numbers 2009QZ09]; the Innovation Engineering Project of Beijing Academy of Science and Technology, China [grant number 23CA001-04].

Ethics statement

This study was reviewed and approved by China University of Mining & Technology-Beijing. All participants provided informed consent to participate in the study. The work described has been carried out in accordance with the Code of Ethics of the World Medical Association Declaration of Helsinki for experiments.

Data availability statement

Data will be made available on request.

CRediT authorship contribution statement

Xiangchun Li: Writing – review & editing, Methodology, Conceptualization. **Yuzhen Long:** Writing – original draft, Data curation. **Chunli Yang:** Visualization, Formal analysis. **Qin Li:** Software, Investigation. **Weidong Lu:** Supervision. **Jiaxing Gao:** Validation,

Software.

Declaration of competing interest

The authors declare that they have no known competing financial interests or personal relationships that could have appeared to influence the work reported in this paper.

Acknowledgment

The authors are deeply grateful to KingFar International Inc. for providing the experimental equipment and technical staff, without whose support this work would never have been possible. We greatly acknowledge the respondents to the questionnaire and the subjects in experiments, who contributed to the data sources for this study. We would also like to express our gratitude to the editors and anonymous reviewers of this paper.

Appendix A. Supplementary data

Supplementary data to this article can be found online at https://doi.org/10.1016/j.heliyon.2023.e20484.

References

[1] E.F. Boadu, C.C. Wang, R.Y. Sunindijo, Characteristics of the construction industry in developing countries and its implications for health and safety: an exploratory study in Ghana, Int. J. Environ. Res. Publ. Health 17 (2020) 4110, https://doi.org/10.3390/ijerph17114110.
[2] M.T. Newaz, P. Davis, M. Jefferies, M. Pillay, The psychological contract: a missing link between safety climate and safety behaviour on construction sites, Saf. Sci. 112 (2019) 9–17, https://doi.org/10.1016/j.ssci.2018.10.002.
[3] B. Shao, Z. Hu, Q. Liu, S. Chen, W. He, Fatal accident patterns of building construction activities in China, Saf. Sci. 111 (2019) 253–263, https://doi.org/10.1016/j.ssci.2018.07.019.
[4] CPWR, Data Reports, 2023, p. 2023. https://www.cpwr.com/research/data-center/data-reports/.
[5] Eurostat, Accidents at Work Statistics, 2022, p. 2023. https://www.sciencedirect.com/science/article/pii/S0925753518309160#b0045.
[6] Statistics Norway, Accidents at Work, 2022, p. 2023. https://www.ssb.no/helse/helseforhold-og-levevaner/statistikk/arbeidsulykker.
[7] P.R.C. Office, Of the Ministry of Housing and Urban-Rural Development, Announcement on the Production Safety Accidents of Housing and Municipal Engineering and Special Governance Actions for Building Construction Safety in 2020, 2022, p. 2023. https://www.mohurd.gov.cn/gongkai/zhengce/zhengcefilelib/202210/20221026_768565.html.
[8] Z. Ma, Statistical analysis of production safety accidents in the field of building construction, Construction and Architecture (2022) 52–55.
[9] M. Fargnoli, M. Lombardi, N. Haber, F. Guadagno, Hazard function deployment: a QFD-based tool for the assessment of working tasks – a practical study in the construction industry, Int. J. Occup. Saf. Ergon. 26 (2020) 348–369, https://doi.org/10.1080/10803548.2018.1483100.
[10] T. Yang, Q. Li, Research on Safety Early-Warning and Management in Works at Heights of Construction Engineering, 2016.
[11] X. Tang, Study on Safety Risk Measurement of Working at Heights in Construction Site and its Application, Southeast University, 2015.
[12] J. Bohm, D. Harris, Risk perception and risk-taking behavior of construction site dumper drivers, Int. J. Occup. Saf. Ergon. 16 (2015) 55–67, https://doi.org/10.1080/10803548.2010.11076829.
[13] M. Zhang, D. Fang, Cognitive causes of construction worker's unsafe behaviors and management measures, China Civ. Eng. J. 45 (2012) 297–305, https://doi.org/10.15951/j.tmgcxb.2012.s2.008.
[14] R.A. Haslam, S.A. Hide, A.G.F. Gibb, D.E. Gyi, T. Pavitt, S. Atkinson, A.R. Duff, Contributing factors in construction accidents, Appl. Ergon. 36 (2005) 401–415, https://doi.org/10.1016/j.apergo.2004.12.002.
[15] L. Cao, X. Zhang, L. Xu, Sampling survey and analysis on consciously unsafe behaviors of building workers, Journal of Jiangsu Jianzhu Institute 15 (8–11) (2015) 21, https://doi.org/10.3969/j.issn.2095-3550.2015.03.003.
[16] S.J. Alper, B.-T. Karsh, A systematic review of safety violations in industry, Accid. Anal. Prev. 41 (2009) 739–754, https://doi.org/10.1016/j.aap.2009.03.013.
[17] J.E. Dodoo, H. Al-Samarraie, Factors leading to unsafe behavior in the twenty first century workplace: a review, Management Review Quarterly 69 (2019) 391–414, https://doi.org/10.1007/s11301-019-00157-6.
[18] D. Fang, C. Zhao, M. Zhang, A cognitive model of construction workers' unsafe behaviors, J. Construct. Eng. Manag. 142 (2016), 4016039, https://doi.org/10.1061/(ASCE)CO.1943-7862.0001118.
[19] B. Shao, Research on Safety Investment Structure Dimensions Ofconstruction Enterprises for Human-Oriented Accidents, 2016.
[20] X. Yang, X. Sun, G. Ren, Analysis of the conscious unsafe behavior of construction workers in multi-party games, Safety & Security 41 (2020) 70–74, https://doi.org/10.19737/j.cnki.issn1002-3631.2020.07.013.
[21] L. Ye, S. Li, Safety Behavior, Tsinghua University Press, Beijing Jiaotong University Press Limited Liability Company, 2005.
[22] K. Li, Research on the Mechanism of Coal Miners' Unsafe Behaviors and its Control Ways, Guide to Business, 2011, pp. 48–50, https://doi.org/10.19354/j.cnki.42-1616/f.2011.11.030.
[23] G. Zhou, W. Cheng, F. Zhuge, W. Nie, Analysis and exploration on correlative theories of man-made errors and human unsafe behaviors, China Saf. Sci. J. (2008) 10–14+176, https://doi.org/10.16265/j.cnki.issn1003-3033.2008.03.009.
[24] M. Fargnoli, M. Lombardi, Preliminary human safety assessment (PHSA) for the improvement of the behavioral aspects of safety climate in the construction industry, Buildings 9 (2019), https://doi.org/10.3390/buildings9030069.
[25] A. Boissy, H.W. Erhard, Chapter 3 - how studying interactions between animal emotions, cognition, and personality can contribute to improve farm animal welfare, in: T. Grandin, M.J. Deesing (Eds.), Genetics and the Behavior of Domestic Animals, second ed., Academic Press, San Diego, 2014, pp. 81–113, https://doi.org/10.1016/B978-0-12-394586-0.00003-2.
[26] S. Zhang, Psychophysiology-Regulation of Consciousness and Control of Physiological Activity, Hunan People's Publishing House, Changsha, 2006.
[27] S. Winge, E. Albrechtsen, B.A. Mostue, Causal factors and connections in construction accidents, Saf. Sci. 112 (2019) 130–141, https://doi.org/10.1016/j.ssci.2018.10.015.
[28] J. Yang, G. Ye, Q. Xiang, M. Kim, Q. Liu, H. Yue, Insights into the mechanism of construction workers' unsafe behaviors from an individual perspective, Saf. Sci. 133 (2021), 105004, https://doi.org/10.1016/j.ssci.2020.105004.

[29] X. Yu, K. Mehmood, N. Paulsen, Z. Ma, H.K. Kwan, Why safety knowledge cannot be transferred directlyto expected safety outcomes in construction workers: the moderating effect of physiological perceived control and mediating effect of safety behavior, J. Construct. Eng. Manag. 147 (2021), 4020152, https://doi.org/10.1061/(ASCECO.1943-7862.0001965.

[30] R. Cai, Research on Influencing Factors of Construction Workers' Intentional Unsafe Behavior, 2018.

[31] J. Zhang, Research on Risky Psychology and ItsImpacts on Flight Risk-Taking Behaviours, 2020.

[32] Y. Ren, Study on the Characteristics of Risk Propensity of Airline Pilots, 2018.

[33] J. Wu, The Research on Safety Risk Tolerance of Construction Workers, 2015.

[34] T. Xiang, Research on the Association of Construction Workers' Fatigue and Unsafe Behavior Based on Physiological Measurement, Tsinghua University, 2019.

[35] L. Wang, S. Gao, Study on eye movement and physiological characteristics of flying risk-taking behaviors, China Saf. Sci. J. 30 (2020) 22–28, https://doi.org/10.16265/j.cnki.issn1003-3033.2020.09.004.

[36] Y. Zhang, Research on the Relationship between Fatigue and Unsafe Behavior Based on Physiological Measurements, 2014.

[37] B. Nie, X. Huang, X. Sun, A. Li, Experimental study on physiological changes of people trapped in coal mine accidents, Saf. Sci. 88 (2016) 33–43, https://doi.org/10.1016/j.ssci.2016.04.020.

[38] R. Doorley, V. Pakrashi, E. Byrne, S. Comerford, B. Ghosh, J.A. Groeger, Analysis of heart rate variability amongst cyclists under perceived variations of risk exposure, Transport. Res. F Traffic Psychol. Behav. 28 (2015) 40–54, https://doi.org/10.1016/j.trf.2014.11.004.

[39] F. Meng, Analysis on Physiological Characteristics of Drivers under Stress, Jilin University, 2018.

[40] J. Healey, J. Seger, R. Picard, Quantifying driver stress: developing a system for collecting and processing bio-metric signals in natural situations, Biomed. Sci. Instrum. 35 (1999) 193–198.

[41] A. Joshi, R. Kiran, A.N. Sah, Stress monitoring through non-invasive instrumental analysis of skin conductivity, Work 57 (2017) 233–243, https://doi.org/10.3233/WOR-172553.

[42] Y. Yu, The Key Methods to Monitor the Safety Status of Construction Workers on Site, 2017.

[43] M. Zhang, Association between Fatigue and Safety Performance of Construction Workers, 2014.

[44] B.K.L. Low, S.S. Man, A.H.S. Chan, The risk-taking propensity of construction workers—an application of quasi-expert interview, Int. J. Environ. Res. Publ. Health 15 (2018) 2250. https://www.mdpi.com/1660-4601/15/10/2250.

[45] H. Meng, Study on the Influence Mechanism of Construction Workers' Risk Perception on Safety Behaviors, 2018.

[46] Z. Ma, Y. Liu, The Determination of the Minimum Sample Size in the Regression Analysis, Statistics & Decision, 2017, pp. 20–22, https://doi.org/10.13546/j.cnki.tjyjc.2017.05.004.

[47] B. Liu, The Surrounding Environment and Implementation Conditions of Construction Site, (2012). https://wenku.baidu.com/view/c5919999bf1e650e52ea551810a6f524cdbfcb3c.html (accessed April 20, 2023)..

[48] Y. Wang, J. Ma, Y. Liu, Analysis of crowd escape behavior in highway tunnel fire environment and multinomial Logit modeling, Journal of Safety Science and Technology 16 (2020) 129–135. https://kns.cnki.net/kcms/detail/11.5335.TB.20201229.0855.002.html.

[49] T. Hao, X. Zheng, H. Wang, K. Xu, S. Chen, Linear and nonlinear analyses of heart rate variability signals under mental load, Biomed. Signal Process Control 77 (2022), 103758, https://doi.org/10.1016/j.bspc.2022.103758.

[50] T. Pan, H. Wang, H. Si, Y. Li, L. Shang, Identification of pilots' fatigue status based on electrocardiogram signals, Sensors 21 (2021) 3003, https://doi.org/10.3390/s21093003.

[51] J. Li, Y. Qin, C. Guan, Y. Xin, Z. Wang, R. Qi, Lighting for work: a study on the effect of underground low-light environment on miners' physiology, Environ. Sci. Pollut. Control Ser. 29 (2022) 11644–11653, https://doi.org/10.1007/s11356-021-16454-1.

[52] J.F. Hair, B. Black, B.J. Babin, R. Anderson, Multivariate Data Analysis: A Global Perspective, Prentice Hall, Upper Saddle River, 2009.

[53] M. Wu, Statistical Analysis of Questionnaires in Practice: Operation and Application of SPSS, Chongqing University Press, Chongqing, 2010.

[54] H.D. Critchley, Review: electrodermal responses: what happens in the brain, Neuroscientist 8 (2002) 132–142, https://doi.org/10.1177/107385840200800209.

[55] N. Hu, C. Chen, J. Yan, Q. Dai, Y. Tang, Z. Quan, Relationship between the anxiety in reactivity stress and physiological psychology indicators for athletes, China Journal of Health Psychology 18 (2010) 824–826.

[56] T.L. Saaty, L.G. Vargas, Decision Making with the Analytic Network Process, Springer, 2006.

[57] Y. Ba, G. Salvendy, W. Zhang, Risk Factors Identification during Driving Based on Behavioral and Physiological Measures, 2015.

[58] G. Borghini, L. Astolfi, G. Vecchiato, D. Mattia, F. Babiloni, Measuring neurophysiological signals in aircraft pilots and car drivers for the assessment of mental workload, fatigue and drowsiness, Neurosci. Biobehav. Rev. 44 (2014) 58–75, https://doi.org/10.1016/j.neubiorev.2012.10.003.

[59] G. Aydogan, R. Daviet, R. Karlsson Linnér, T.A. Hare, J.W. Kable, H.R. Kranzler, R.R. Wetherill, C.C. Ruff, P.D. Koellinger, G. Nave, B.I.G.B. Consortium, Genetic underpinnings of risky behaviour relate to altered neuroanatomy, Nat. Human Behav. 5 (2021) 787–794, https://doi.org/10.1038/s41562-020-01027-y.

[60] S.J. DeWitt, S. Aslan, F.M. Filbey, Adolescent risk-taking and resting state functional connectivity, Psychiatry Res. Neuroimaging. 222 (2014) 157–164, https://doi.org/10.1016/j.pscychresns.2014.03.009.

[61] Y.I. Deza Araujo, S. Nebe, P.T. Neukam, S. Pooseh, M. Sebold, M. Garbusow, A. Heinz, M.N. Smolka, Risk seeking for losses modulates the functional connectivity of the default mode and left frontoparietal networks in young males, Cognit. Affect Behav. Neurosci. 18 (2018) 536–549, https://doi.org/10.3758/s13415-018-0586-4.

[62] S. Baltruschat, A. Cándido, A. Megías, A. Maldonado, A. Catena, Risk proneness modulates the impact of impulsivity on brain functional connectivity, Hum. Brain Mapp. 41 (2020) 943–951, https://doi.org/10.1002/hbm.24851.

[63] E. Barkley-Levenson, F. Xue, V. Droutman, L.C. Miller, B.J. Smith, D. Jeong, Z.-L. Lu, A. Bechara, S.J. Read, Prefrontal cortical activity during the stroop task: new insights into the why and the who of real-world risky sexual behavior, Ann. Behav. Med. 52 (2018) 367–379, https://doi.org/10.1093/abm/kax019.

[64] T. Raij, A. Nummenmaa, M.-F. Marin, D. Porter, S. Furtak, K. Setsompop, M.R. Milad, Prefrontal cortex stimulation enhances fear extinction memory in humans, Biol. Psychiatr. 84 (2018) 129–137, https://doi.org/10.1016/j.biopsych.2017.10.022.

[65] R. Cools, M. D'Esposito, Inverted-U–Shaped dopamine actions on human working memory and cognitive control, Biol. Psychiatr. 69 (2011), https://doi.org/10.1016/j.biopsych.2011.03.028 e113–e125.

[66] K.A. Zalocusky, C. Ramakrishnan, T.N. Lerner, T.J. Davidson, B. Knutson, K. Deisseroth, Nucleus accumbens D2R cells signal prior outcomes and control risky decision-making, Nature 531 (2016) 642–646, https://doi.org/10.1038/nature17400.

[67] Knowing Neurons, Why Dopamine Makes People More Impulsive, WordPress. (2016). https://knowingneurons.com/blog/2016/03/10/dopamine-makes-people-impulsive/(accessed April 21, 2023)..

[68] Knowing Neurons, Why Dopamine Makes People More Impulsive, WordPress, 2016.

[69] C. Tronstad, H. Kalvøy, S. Grimnes, Ø.G. Martinsen, Waveform difference between skin conductance and skin potential responses in relation to electrical and evaporative properties of skin, Psychophysiology 50 (2013) 1070–1078, https://doi.org/10.1111/psyp.12092.

[70] Y. Tai, K. Obayashi, Y. Yamagami, K. Saeki, Inverse association of skin temperature with ambulatory blood pressure and the mediation of skin temperature in blood pressure responses to ambient temperature, Hypertension 79 (2022) 1845–1855, https://doi.org/10.1161/HYPERTENSIONAHA.122.19190.

[71] J. Kitazono, Y. Aoki, M. Oizumi, Bidirectionally connected cores in a mouse connectome: towards extracting the brain subnetworks essential for consciousness, Cerebr. Cortex 33 (2023) 1383–1402, https://doi.org/10.1093/cercor/bhac143.

[72] C. Xue, L.E. Kramer, M.R. Cohen, Dynamic task-belief is an integral part of decision-making, Neuron 110 (2022) 2503–2511.e3, https://doi.org/10.1016/j.neuron.2022.05.010.

[73] G.K. Uyanık, N. Güler, A study on multiple linear regression analysis, Procedia Soc Behav Sci 106 (2013) 234–240, https://doi.org/10.1016/j.sbspro.2013.12.027.

[74] T. Nyitrai, M. Virág, The effects of handling outliers on the performance of bankruptcy prediction models, Socioecon Plann Sci 67 (2019) 34–42, https://doi.org/10.1016/j.seps.2018.08.004.

[75] Z. Wu, Age difference of search time in short-term meniory and the relation between search time and arousal level, Acta Psychol. Sin. (1988) 150–158.
[76] X. Li, Drivers' hazard perception based on eye movement, Automobile Applied Technology 47 (2022) 29–34, https://doi.org/10.16638/j.cnki.1671-7988.2022.007.007.
[77] X. Ying, Research on Emotion Recognition Based on Multiple Physiological Signals, Nanjing University of Posts and Telecommunications, 2017.

Notation

The following symbols are used in this paper

t: Time during consciously unsafe behavior
y_1: Skin conductance during consciously unsafe behavior
y_2: Inter-beat interval during consciously unsafe behavior
y_3: Respiration rate during consciously unsafe behavior
y_4: Skin temperature during consciously unsafe behavior
x_1: Task-related risk perception of workers
x_2: Hazardous attitude of workers
x_3: Variation of skin conductance of workers
x_4: Variation of inter-beat interval of workers
x_5: Variation of skin temperature of workers
y: Unsafe behavior performance score